2011

Ultra-Low Power Electronics for Autonomous Micro-Sensor Applications

Rebeka Davidova
University of South Florida, rm.dova@gmail.com

Ultra-Low Power Electronics for Autonomous Micro-Sensor Applications

by

Rebeka Davidova

A thesis submitted in partial fulfillment
of the requirements for the degree of
Master of Science in Electrical Engineering
Department of Electrical Engineering
College of Engineering
University of South Florida

Major Professor: Thomas M. Weller, Ph.D.
Gokhan Mumcu, Ph.D.
Jing Wang, Ph.D.

Date of Approval:
March 21, 2011

Keywords: lock-in amplifier, sensor network, frequency doubling reflectenna, diode
doubler, conversion efficiency

DEDICATION

This thesis is dedicated to the most incredible woman I know. She is a

woman whose commitment to her children takes precedence above all else

in her life. She has a spirit of selfless devotion and of endless compassion.

Her presence is soft and her eyes show kindness.

This is for my mother, Michele.

ACKNOWLEDGEMENTS

I wish to acknowledge Dr. Thomas Weller for his guidance, his generous time, and for encouraging me to find the "why" in every aspect of my work. I was incredibly fortunate to have the opportunity to become part of the USF-WAMI group, and the experiences I have gained are invaluable. I would also like to thank my committee members, Dr. Gokhan Mumcu and Dr. Jing Wang.

I would like to acknowledge all those who have helped me along this journey: Bojana, my sister, for your endless support, honest advice, and selfless friendship; my dear Chami, my first real friend in Tampa - I will never forget our afternoon walks, your amazing Sri Lankan cooking and our time in Turino, Italy; Yohannes, for your countless motivational speeches and loyal friendship - I will never forget Chapter Two; SBS, for teaching me to sit by the river of thoughts - your positive words and creativity made me smile; QB, for your inspiring words and uplifting spirit; David (Il Maestro) for your lovely serenades in the middle of the day and for always making me laugh regardless of my mood; my dear Ebenezer, one of the most caring people I know - I will never forget the chocolate bar; all those in my 412 family who never hesitated to offer a helping hand: Ibrahim Nassar, Tony Price, Scott Skidmore, Evelyn Banabe, Michael Grady, and Maria Cordoba.

Special thanks are due to my professors who have guided and formed my understanding of RF, a subject that has become close to my heart.

TABLE OF CONTENTS

LIST OF TABLES

LIST OF FIGURES

iv

v

ABSTRACT

This thesis presented the research, design and fabrication associated with a unique application of rectenna technology combined with lock-in amplification. An extremely low-power harmonic transponder is conjoined with an interrogator base-station, and utilizing coherent demodulation the Remote Lock-In Amplifier (RLIA) concept is realized. Utilizing harmonic re-radiation with very low-power input, the 1st generation transponder detects a transmitted interrogation signal and responds by retransmitting the second harmonic of the signal. The 1st generation transponder performs this task while using no additional power besides that which accompanies the wireless signal. Demonstration of the first complete configuration provided proof of concept for the RLIA and feasibility of processing relevant information under "zero" power operating conditions with a remote transponder.

Design and fabrication of a new transponder where the existing zero-bias transponder was modified to include a DC bias to the diode-based frequency doubler is presented. Applied bias voltage directly changed the impedance match between the receiving 1.3 GHz antenna and the diode causing a change in conversion loss. Testing demonstrated that a change in conversion loss induces an amplitude modulation on the retransmission of the signal from the transponder. A test of bias sweep at the optimal operating frequency was performed on the 2nd generation transponder and it was seen that

a change of ~ 0.1 V in either a positive or negative bias configuration induced an approximate 15 dB change in transponder output power.

A diode-integrated radar detector is designed to sense microwaves occurring at a certain frequency within its local environment and transform the microwave energy to a DC voltage proportional the strength of the signal impinging on its receiving antenna. The output of the radar detector could then be redirected to the bias input of the 2nd generation transponder, where this DC voltage input would cause a change in conversion loss and modulate the retransmitted interrogation signal from the transponder to the base station. When the base station receives the modulated interrogation signal the information sensed by the radar detector is extracted. Simulations and testing results of the fabricated radar detector demonstrate capability of sensing a signal of approximately -53.3 dBm, and accordingly producing a rectified DC voltage output of 0.05 mV. A comparison is made between these findings and the transponder measurements to demonstrate feasibility of pairing the radar detector and the 2nd generation transponder together at the remote sensor node to perform modulation of interrogation signals.

CHAPTER 1

INTRODUCTION

There is no argument that radio has made a profound impact on humanity over the past hundred years. Some of the primary applications of this technology have been within the realm of mobile and telecommunications, navigation, and links for computer-controlled systems. Advances continue to be made, particularly within microwave technology, involving new applications. Microwave power transmission was the desired application behind the conception of the "rectenna" in the mid 1960's [1], and since that time rectenna technology has continued to develop. New arenas have been discovered for this technology and methods of use have expanded, including remote sensing [2], monitoring of infrastructure [3], and energy harvesting and recycling [4, 5].

The research described in this thesis focuses on a unique application of sensing involving rectenna technology combined with phase sensitive detection implemented by a lock-in amplifier within an interrogating transceiver. A harmonic re-radiator is employed within the system as a remote sensor and signal interrogation is performed to communicate relevant information from its location. The goal of this research is to implement phase sensitive detection to enhance the ability of the interrogating transceiver to detect a very low power return signal from the remote sensor.

1.1   Lock-In Amplifiers and Phase Sensitive Detection

Lock-in amplifiers are devices used to detect extremely small AC signals reaching as low as -100 dBm or more. It is not uncommon for lock-in amplifiers to operate with sensitivities in the nano-volt range, allowing for monitoring and extracting of information below the system noise floor. Lock-in amplifiers have long been used in laboratories for accurate small signal detection and complex impedance measurement [6-8].

The technique employed by lock-in amplifiers to perform such tasks is referred to as "phase-sensitive detection" and entails singling out a signal component at a specific reference frequency. Noise signals at all other frequencies are rejected by the lock-in amplifier and thus do not contribute to the measurement. Phase sensitive detection is performed by the lock-in amplifier by utilizing a phased locked-loop that synchronizes to the external reference channel input (Figure 1.1) creating an internal reference signal. This internal reference signal is then multiplied by the signal channel input. The product of the two signals is amplified and passed through a low-pass filter, removing the AC components. The resulting signal will be zero unless the signal frequency is identical to the reference frequency, in which case a DC voltage proportional to the signal channel input will be seen at the lock-in amplifier's output (DC Out in Figure 1.1) [9].
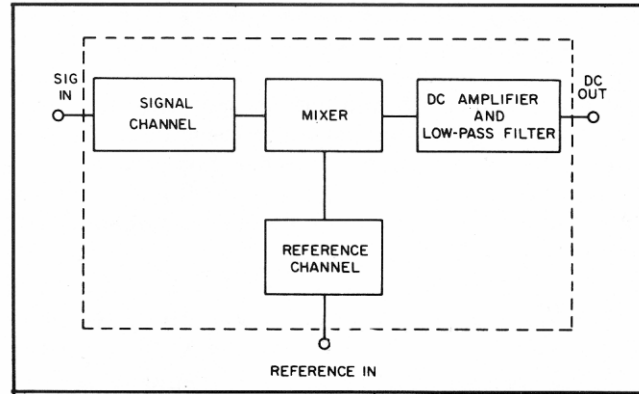
Figure 1.1: Block diagram of Lock-In Amplifier

With the goal of implementing phase sensitive detection with a lock-in amplifier in a remote fashion, the proposed scheme in Figure 1.2 was created. The scheme utilizes a lock-in amplifier within an interrogating base station (interrogator node) and a low- to zero-power transponder as part of the remote sensor node. The configuration is named a Remote Lock-In Amplifier (RLIA) and it is unique in that the high power consuming electronics within the RLIA system are separated from the low-power remote components, while the system as a whole performs phase sensitive detection to sense and gather remote intelligence.
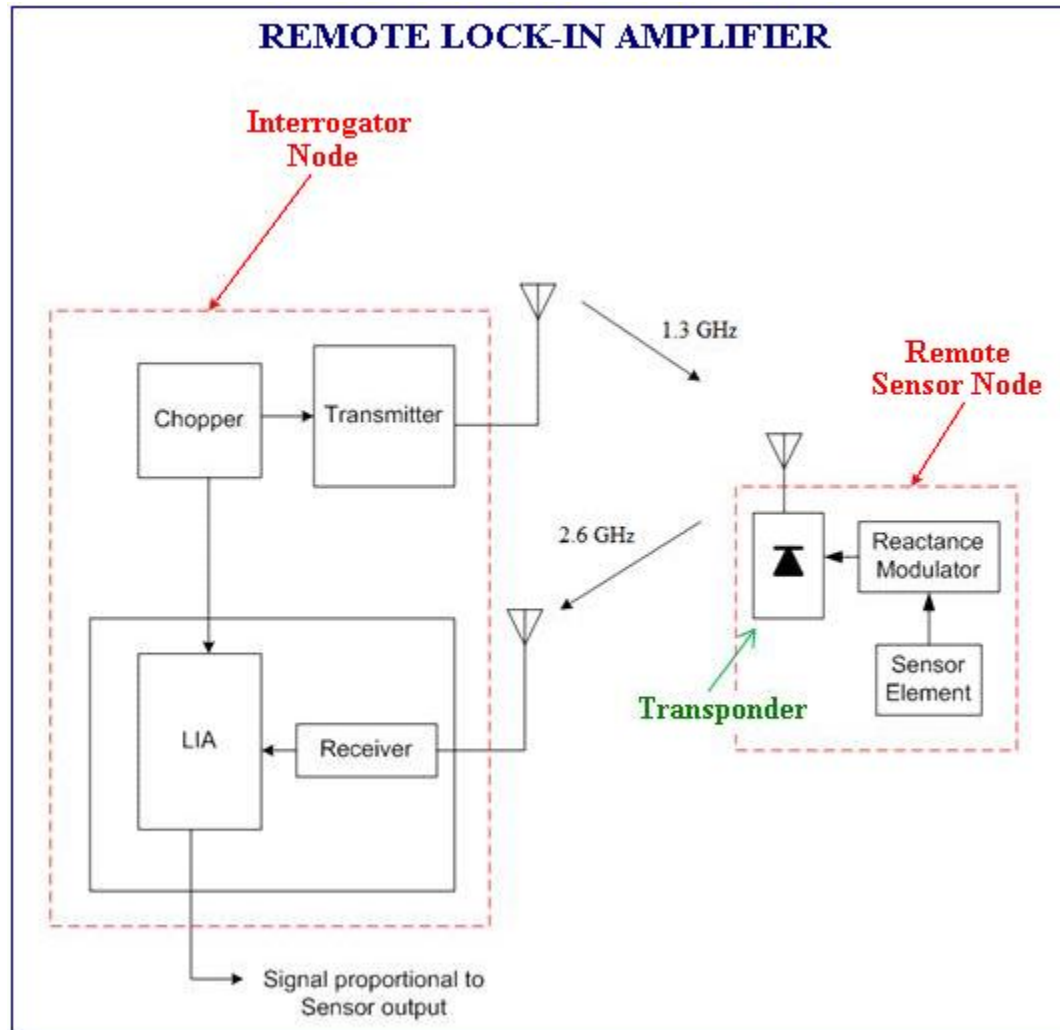
Figure 1.2: Block diagram of RLIA concept.

1.2   Harmonic Re-Radiator: 1st and 2nd Generation

Employed within the RLIA system is a harmonic re-radiator, referred to as a Frequency Doubling Rectenna (FDR). The FDR was developed for low-power sensing applications [2]. An illustration of the FDR concept is depicted in Figure 1.3. Using the principles of frequency multiplication, this device receives an interrogation signal at 1.3 GHz and retransmits the 2nd harmonic at 2.6 GHz. The FDR is initially used in the first stage of demonstrating the RLIA concept by assuming the role of the transponder or remote sensor node. The printed circuit board design consists of two quarter-wavelength patch antennas (1.3 GHz and 2.6 GHz) and a diode-based doubler. The FDR was designed for minimum conversion loss for a low-power input application, yet possesses sufficient sensitivity for efficient data collection within a remote interrogation scheme.
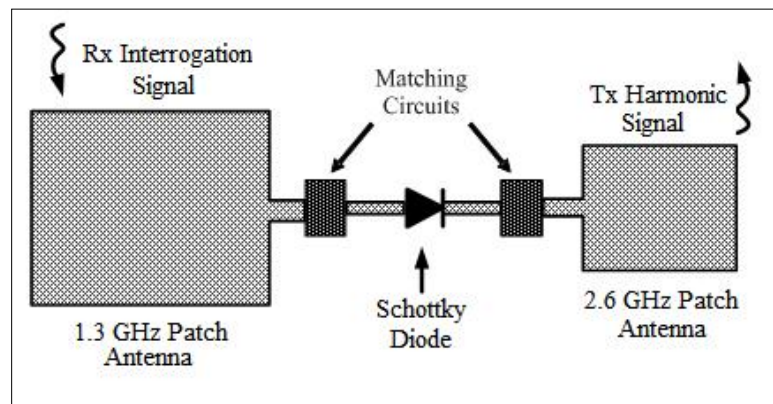
Figure 1.3: Concept of Frequency Doubling Rectenna [2]. (1st generation transponder)

5

The goal in the first phase of this research involved verifying the capability to effectively communicate with the 1st generation low-power remote transponder within the RLIA system. The Interrogator (RLIA) from Figure 1.2 was constructed using standard testing equipment and testing was performed at a distance between the interrogating node and remote sensor node that would provide an input power giving the best possible conversion efficiency from the transponder (Chapter Three, Figure 3.7, Appendix A). Sweeps of transmitted power and frequency were performed to characterize the 1st generation transponder and determine the minimum detectable signal level arriving to the interrogator node from the remote sensor node. The entire RLIA system was characterized through measured link budgets, which were then verified with the calculated link budgets.

The second phase of implementing the RLIA system involved a redesign of the 1st generation transponder to include a DC bias connection to the diode doubler, as seen in Figure 1.4 (2nd generation transponder). An applied bias voltage to the diode directly changes the impedance match between the receiving 1.3 GHz antenna and the doubler causing a change in conversion loss. This change in conversion loss will induce an amplitude modulating effect on the retransmission of the signal from the transponder by reducing the output power of the processed signal. Ideally, a small change in bias voltage will cause a decrease or increase in the output power of the transponder to essentially turn "off" or "on" the retransmitted signal. Testing was performed according to the diagram seen in Figure 3.10 of Chapter Three (Appendix A), and it was verified that the new design in fact could process relevant information back to the interrogator node through this modulation process. Such tests provided the initial proof of concept for utilizing the

6

RLIA system with a frequency discrimination scheme where a remote network of several devices could be interrogated simultaneously and each individual device communicates detected information back to a base station relevant to its environment.
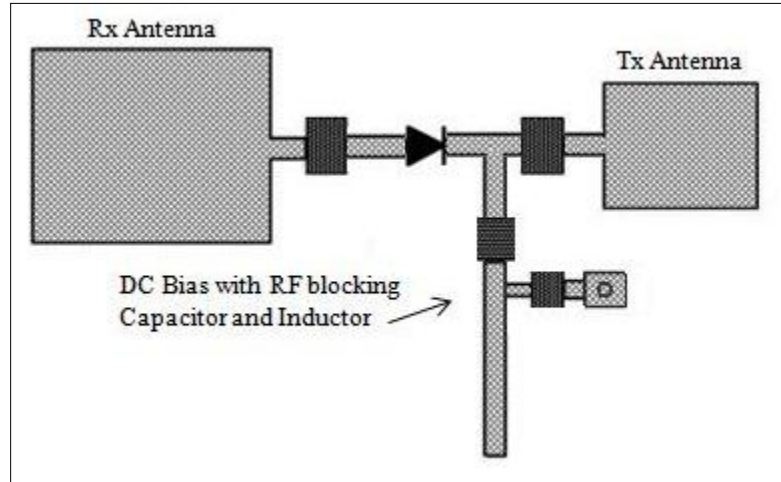
Figure 1.4: Concept of biased transponder (2nd generation transponder).

1.3   Diode-Integrated Radar Detector

In the final stage of this research a diode-integrated radar detector is designed, fabricated and tested. Providing the functionality of the sensor element and reactance modulator as seen in Figure 1.2, the radar detector verifies feasibility of using a separate device concurrently with the 2nd generation transponder to realize the full RLIA system. As seen in Figure 1.5, the radar detector is designed by modifying the 1st generation transponder and replacing the transmitting 2.6 GHz patch antenna with a pad for a DC voltage connection. Additionally, a shunt capacitor is introduced to short the RF components of the signal, and a shunt resistor is included to maximize voltage sensitivity.

7

Being essentially a rectenna, the radar detector senses microwaves occurring at a certain frequency within its local environment and transforms the microwave energy to a DC voltage proportional the strength of the signal impinging on the receiving antenna. The output of the radar detector could then be redirected to the bias input of the 2nd generation transponder, where this DC voltage input would cause a change in conversion loss and modulate the retransmitted interrogation signal to the base station. When the base station receives the modulated interrogation signal—using the lock-in amplifier—the information sensed by the radar detector will be extracted. However, when the radar detector is not sensing the presence of microwave energy at the frequency of interest it will simply have a zero DC voltage output, which will not affect the conversion efficiency of the transponder.

Figure 1.5: Concept of diode-integrated radar detector

1.4   Overview and Contributions of the Research

The primary goals of this research were:

- Develop using standard testing equipment and the 1st generation transponder the RLIA system, and demonstrate the capability to effectively communicate with the low-power sensor.

- Design, fabricate and test the 2nd generation transponder and verify modulation capabilities using the same RLIA system.

- Design, fabricate and test a diode-integrated radar detector to determine feasibility of employing such a device with the 2nd generation transponder to effectively communicate information sensed within the environment of the remote sensor node (Figure 1.2).

Chapter Two presents background research related to rectennas and various applications and well as an introduction to the 1st generation transponder (harmonic re-radiator) used within the RLIA system. Chapter Three focuses on characterization of the various components of the RLIA system and integration of the transponder within the system. The second part of Chapter Three presents the design and fabrication of the 2nd generation transponder. Test results are presented to verify the feasibility of using the transponder in the RLIA system to implement a frequency discrimination communication scheme. Chapter Four presents the design and fabrication of a diode-integrated radar detector to investigate feasibility of introducing a separate sensing element and utilizing it concurrently with the 2nd generation transponder. The ultimate goal in this research is to have the two devices comprise a remote sensor node and provide the initial proof of

9

concept where information occurring at a specific frequency is detected and this is communicated back to the interrogator node in the form of a modulated interrogation signal.

CHAPTER 2

BACKGROUND OF RECTENNAS, SIGNIFICANCE IN CURRENT WORK AND RELATED RESEARCH

2.1   Introduction

Rectennas have assumed a pivotal role in the growing field of low-power sensing and monitoring, where small passive devices are needed that fulfill cost, size, weight and power issues. Additionally, rectenna arrays show significant promise for the continued development of wireless power transfer, and the exploration of this concept within new arenas has demonstrated a potentially bold impact on future technologies.

Within this chapter, a discussion of rectenna technologies is presented and some of the many applications are explored. Beginning with a brief look at the history of wireless microwave power transfer, this chapter investigates related applications to Solar Power Satellites (SPS), aircraft powering, and wireless power distribution systems in buildings. Rectenna array technologies for various applications are also discussed, including the different antenna polarizations employed, choices of diodes, and operational parameters.

Applications within wireless sensor networks are then presented, focusing on retrodirective array systems and their use within sensor networks, monitoring and sensing of infrastructure, and energy harvesting and recycling. Lastly, a Frequency Doubling Rectenna (FDR) used as a harmonic re-radiator is described as another application of rectenna technology for sensing purposes. It is the subject of further discussion

11

throughout this thesis and is redesigned and employed within a transponder-based interrogation network scheme.

2.2   Diode Applications and Schottky Diodes

Because a diode is a non-linear circuit element, it will generate harmonics of a given sinusoidal input signal. According to Balanis, this non-linearity may be exercised to provide useful applications of signal detection, demodulation, switching, frequency multiplication, and oscillation [10]. Frequency conversion is a common application of the Schottky barrier diode, and as noted in [11] encompasses signal detection (demodulation of an amplitude modulated signal), mixing (frequency shifting), and rectification (conversion of an AC to DC signal). As most wireless sensor devices perform at least one of the aforementioned tasks, a Schottky diode is a commonly used element in the design of such devices. For high frequency applications, a Schottky diode is preferable to the classic *pn* junction diode. As opposed to the *pn* junction diode, the Schottky diode consists of a semiconductor-metal junction that maintains a much lower junction capacitance and forward voltage drop, providing better conversion efficiency.

2.3   Schottky Diode Characteristics and Application Specific Parameters

As a common application of diodes, rectification is used for signal strength indication. As previously discussed, and also cited in [4], within low RF frequencies (kHz to lower MHz), both *pn* diodes and transistors are used as rectifiers. However, at microwave frequencies (1 GHz and higher), either GaAs or Si Schottky diodes are necessary, due to the required transit times.

Within a rectifier application such devices convert a fraction of a RF signal to DC power. The result of this conversion is seen as an output of the diode in the form of a DC voltage proportional to the input signal. Let the diode voltage be equal to $V=V_0+v$, where the DC bias voltage is V_0 and the small AC signal voltage is v. The diode current can be expressed in expanded Taylor series form as the sum of the DC bias current, I_0, and the AC current, *i, as*:

$$I(V) = I_0 + i = I_0 + VG_d + \frac{v^2}{2}G'_d + \cdots \qquad (2.1)$$

where the bias current is $I_0=I(V_0)$, and G_d is the dynamic conductance of the diode, where $G_d = \dfrac{1}{R_j}$ and R_j is the junction resistance. In practice, the AC characteristics of a diode involve reactive effects due to the structure and packaging of the diode. Figure 2.1 shows an equivalent AC circuit model for a Schottky diode.
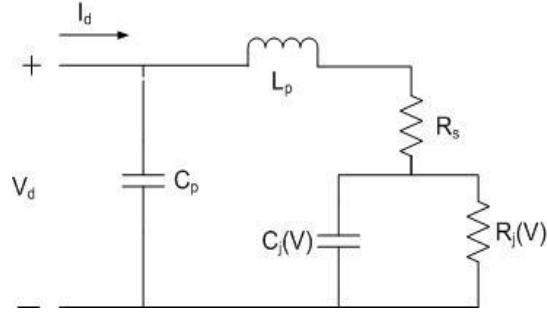
Figure 2.1: Equivalent AC circuit model for a Schottky diode.

If the diode voltage is comprised of a sinusoidal small-signal RF voltage and a DC bias voltage, it will be equal to:

$$V = V_0 + v_0 \cos \omega_0 t \tag{2.2}$$

Therefore, equation (2.1) can be rewritten as:

$$I = I_0 + V G_d \cos \omega_0 t + \frac{v^2}{2} G'_d \cos^2 \omega_0 t \tag{2.3}$$

$$= I_0 + \frac{v^2}{4} G'_d + V G_d \cos \omega_0 t + \frac{v^2}{4} G'_d \cos 2\omega_0 t \tag{2.4}$$

where I_0 is the bias current and $\dfrac{v_0^2 G'_d}{4}$ is the DC rectified current. Additionally, and due to inherent non-linearity of the diode element, the output of the diode will produce

14

harmonics of ω_0, $2\omega_0$, and higher order. Often times, for the purposes of signal detection, harmonics produced by circuit elements will be removed by a simple low-pass filter. However, in some applications of remote sensing, the production of these signal harmonics are put to use, as seen in [2]. Two important parameters in the application of signal detection for a diode are current sensitivity, β_i, and voltage sensitivity, β_v. Current sensitivity for a diode is defined as the change in DC output current due to a given RF power input from the received signal. Following from (2.1), using the first term in the sum, the RF power input to the diode is $\frac{v_0{}^2 G_d}{2}$. Additionally, (2.4) shows that the change in DC current will be $\frac{v_0{}^2 G'_d}{4}$. Therefore, the current sensitivity can be defined as:

$$\beta_i = \frac{\Delta I_{DC}}{P_{IN}} = \frac{G'_d}{2G_d}\left(\frac{A}{W}\right) \qquad (2.5)$$

Voltage sensitivity, β_v, can be defined in terms of the voltage drop across the junction resistance when the diode is open-circuited as:

$$\beta_v = \beta_i R_j \qquad (2.6)$$

Voltage sensitivity is quantified in units of $\frac{mV}{mW}$, and a typical diode detector will range from 400 to 1500 $\frac{mV}{mW}$, as seen in [11].

15

An area of concern associated with the Schottky diode—especially within the applications of detection and wireless power transfer—is the loss occurring inside the element itself, which inevitably contributes to circuit loss and overall device efficiency. Such losses are associated with the voltage drop of the Schottky barrier and the series resistance of the diode. As noted in [12], a significant reduction in diode series resistance can be achieved during the design process of the substrate, active epitaxial region, and diode contacts.

For some detecting applications, a diode is employed to demodulate an amplitude modulated RF signal. In this case, the diode voltage can be expressed as:

$$V(t) = V_0(1 + mcos\omega_m t)cos\omega_0 t \quad (2.7)$$

where ω_0 is the RF carrier frequency and ω_m is the modulated frequency. The output spectrum of the detected amplitude modulated signal can be seen in Figure 2.2, where the linear output terms of the diode voltage have frequencies of ω_0 and $\omega_0 \pm \omega_m$.

16
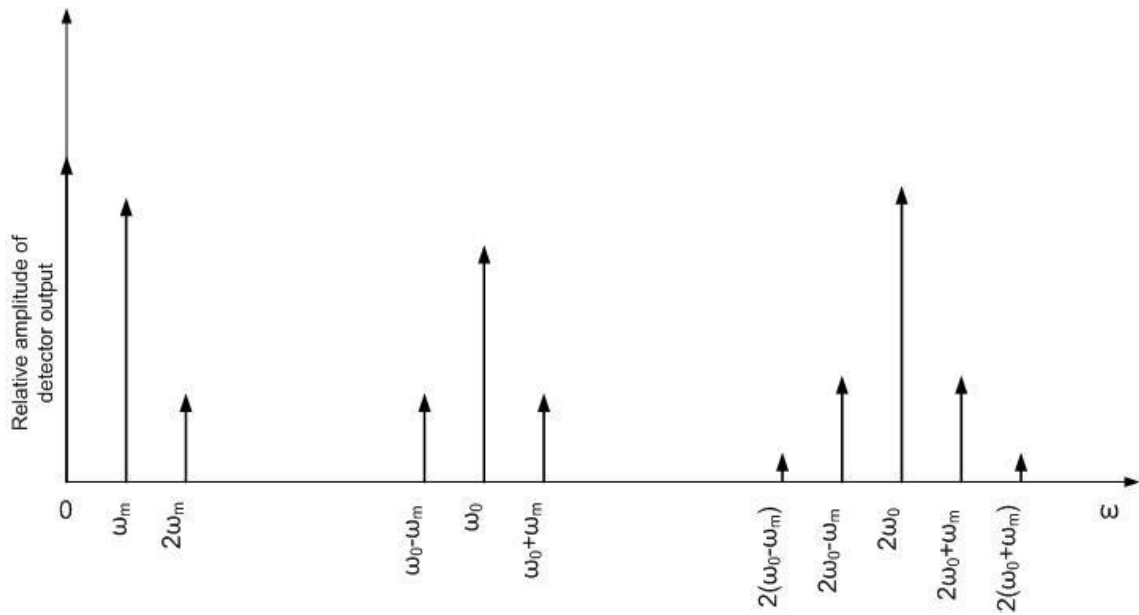
Figure 2.2: Spectral output of detected modulated signal

Table 2.1 shows the frequencies and relative amplitudes of the terms of the diode output that are proportional to the square of the diode voltage. Square-law behavior from the output of a diode detector is limited and can only be obtained within a certain region of input powers.

17

Frequency	Relative Amplitude
0	$\dfrac{1+m^2}{2}$
ω_m	$2m$
$2\omega_m$	$\dfrac{m^2}{2}$
$2\omega_0$	$\dfrac{1+m^2}{2}$
$2\omega_0 \pm \omega_m$	m
$2(\omega_0 \pm \omega_m)$	$\dfrac{m^2}{4}$

Outside of this region—where input signal power levels are either too large or too small—the square-law region is not applicable. If the input signal power level is too large, the diode output will become saturated, approaching a linear and then constant i versus P characteristic. In the opposite regard, if the input signal power level is too small it will be lost within the noise floor, becoming undetectable. Figure 2.3 shows a typical voltage sensitivity curve for a diode. Within the square-law region, $V_{out} \sim V_0{}^2 \sim P_{in}$. In

applications where power levels are interpreted by the output voltage provided by the diode, the square-law region of operation is essential [11]. Some examples of diode applications of this type can be seen in [13], [14], and [4].

For the purposes of optimized diode sensitivity or to generate modulation characteristics, a bias voltage may be applied to the diode. At a certain operating voltage, a diode may either produce its maximum output or it may reduce its output by a sufficient amount that it may serve as a "digital off" state for modulation purposes.
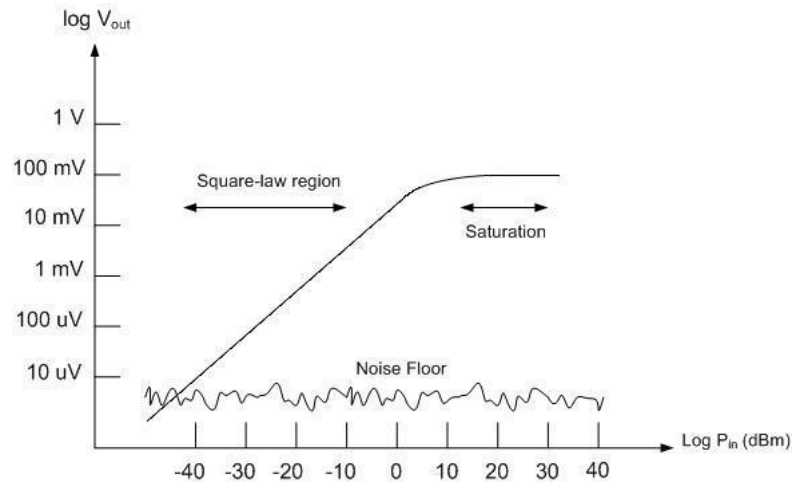
Figure 2.3: Square-law region of a diode detector

As seen in [15], wherein a diode is utilized to generate the second harmonic of a received interrogation signal, maximum radiation is achieved in the on-state when a varactor diode is operating under reverse-bias. Signal transmission is then reduced by approximately 10 dB when the applied bias changes to 0 V.

19

2.4   Wireless Power Transfer as an Application of Diode Rectification

At the end of the nineteenth century Nicola Tesla conceived the idea of transmitting electrical power without wires [16]. He worked for years on a concept that would employ the Earth and Ionsphere as a giant capacitor, storing energy that would be distributed by means of wireless power transmission. Unfortunately, due to a fateful decision by Tesla's investor, J. P. Morgan—after learning the project was designed for wireless power transmission and not for the purpose of telegraphy—the work was abandoned. It is unknown if the project could have achieved the potential success Tesla believed it would. Interestingly, for the majority of the twentieth-century, radio had been used primarily as a means of transmitting information and intelligence, seemingly being disregarded for the purposes of power transmission—perhaps due to the lack of necessary microwave technology [17]. After the invention and initial development of microwave technologies, usage was predominantly limited to communications and radar.

In the most elementary fashion, wireless power transmission can be defined as a three-stage process. The first step involves conversion of DC electrical power to RF power. Secondly, the RF power is transmitted through space to specific location. The third step then involves capturing the RF power through a reception device and converting it back to DC power through a receiver system [1]. Wireless power transmission has been employed in a vast array of applications including helicopter and airplane powering [17][18], solar powered satellite-to-Earth transmission of microwave energy [19], nonlinear plasma-wave excitation in the ionosphere by high-power microwave beams [17], and microwave power transmission for wireless power distribution systems in buildings [20].

20

2.4.1 Development of Microwave Power Transmission (MPT) and Conception of the "Rectenna"

By the early 1960s, work done by R. H. George at Purdue showed that dense arrays of closely spaced diodes within an expanded waveguide could achieve as much as 40 W of DC power output from microwaves in the range 2-3 GHz [21]. Prior to this point, the semiconductor diode had been ignored as a microwave power rectifier due to its individual inherently low-power handling capability. Consequently, this work demonstrated how power-handling capability could be combined to produce reasonable amounts of DC power. However, one issue still to be resolved at that time was the problem relating to low RF power collection efficiency. As a solution to the limiting potential of the first diode array power rectifiers, the concept of the "rectenna" was born [1]. The proposed solution to the low efficiency of the prior work was to remove the individual full-wave rectifiers from the waveguide, incorporate them with half-wave dipoles, and introduce a reflecting plane behind them [22]. In an effort to drive a proposed microwave-powered helicopter experiment—that later developed into a contract between Raytheon and the Air Force—the development of the rectenna continued [1]. The outcome was the first rectenna array, conceived at Raytheon in 1963 and built and tested at Purdue. It was composed of 28 half-wave dipoles, and each was terminated in a bridge rectifier comprised of four IN82G point-contact, semiconductor diodes [23].

The development of a microwave beam powered helicopter at Raytheon accelerated the evolution of rectenna technology and was a pivotal experiment in the further study of free-space microwave power transfer. The microwave-powered helicopter was essentially a hovering platform with an electric motor, a propeller, and a 4

21

ft^2 rectenna array. The rectenna array was assembled from 4480 semiconductor IN82G diodes and had a maximum power output of 270 Watts. The microwave power source employed was a 5 kW magnetron that operated at 2450 MHz. Combined capture and rectification efficiency of the rectenna array was significant, reaching levels of 55 percent, with rectification efficiencies of the diodes themselves being measured at 80 percent. Additionally, the helicopter flew continuously for an impressive 10 hours at an altitude of 50 feet. The helicopter device demonstrated an unmanned propulsion technology that could be sustained by a continuous supply of "weightless fuel," and could serve as a useful tool in the area of communication and surveillance [18].

Following the success of the helicopter project, Brown (et al) published findings from continued research in power reception efficiency in free-space with rectifier devices as seen in [12]. Rectennas were designed using GaAs Schottky-barrier diodes combined with rectifier circuit technology and input and output filtering, reaching 82-86 percent RF-to-DC efficiency—the highest recorded RF-to-DC conversion efficiency according to Matsumoto [17]. A single-diode half-wave rectifier configuration was the focus of the continued work, as it was believed to embody an agreeable compromise between efficiency, power handling capability, cost, and printed circuit adaptation. Additionally, GaAs diodes were specifically used because of their ability to individually supply 5-10 W of DC power output when used in a rectenna element.

Further development of the rectenna was conducted with a focus on the design of low-power density operation. As seen in [24], a 2.45 GHz rectenna was designed to absorb small amounts (as low as 50 mW) of microwave power. This rectenna had the capacity to absorb incident power density levels that were 10,000 times lower than

22

contemporary rectennas and convert the power into DC at levels that were still useful. To achieve this, the standard rectenna design—in which there was an individual rectifier in each microwave collecting element—was abandoned. A broadside array was adopted as the collecting aperture and several advantages were realized, a few of which were: (1) the ability to filter out harmonics by introducing a filter element, (2) a reduction in the number of required diodes, (3) maximum efficiency realized from the diodes, and (4) the ability to employ the array as either a transmitter or receiver [24].

Continuing forward with Brown's findings from the original helicopter experiment, Matsumoto published [17], where a project named MILAX is described—a fuel-free microwave driven airplane equipped with lightweight microstrip rectennas. In order to control a target moving both vertically and horizontally with a microwave power beam, a phased-array transmitting antenna was designed.

2.4.2 MPT in Solar Power Satellites (SPS) and Related Experiments

Over the years, since the beginning of rectenna technology, research and advances have been made within the subject of rectennas used in free-space microwave power transfer. One area of particular interest is solar power satellites (SPS). Solar power satellites, which are geostationary orbital stations, are characterized by having immense power capacity (5-GW). Such satellites generate electrical power through solar cells and transmit microwaves from the station to a site on Earth composed of rectenna arrays. SPS, a concept introduced by Dr. Peter Glaser of the Arthur D. Little Company in 1968 [25], was a development that was predicted by Brown to have a profound effect on the future direction of wireless power transfer technology. Many key issues stemming from

23

the technology of SPS became apparent to Glaser, and in [26] he addresses the economic and environmental considerations directly related to the microwave beaming utilized in MPT for SPS.

In collaboration, Brown and Glaser organized the first technical session on SPS at the International Symposium of the International Microwave Power Institute at the Hague in 1970. In a joint effort between NASA, JPL and Raytheon in 1973 at Raytheon's Goldstone facility, the first long distance wireless power transfer experiment using SPS technology was demonstrated. Power was transferred by a microwave beam over a distance of 1 mile, with a DC output of 30 kW, utilizing a 288 ft^2 rectenna array [1]. It was a significant milestone in the progress of SPS technology, as the distance and amount of power transfer documented were almost two orders of magnitude greater than had been accomplished in prior experiments. In 1976-77 important electrical and mechanical improvements were made to rectenna technology through work supported by LeRC. One of the most significant changes was the move from a three-plane system to a two-plane system; this new format would eventually lead to thin-film etched circuit format used in aerospace applications [1], [27]. Brown further focused his research and work of high-powered rectennas toward SPS applications, later publishing [28].

Through the years, since the conception of SPS, research has continued in this technology. In 1995, Shinohara and Matsumoto developed a new rectenna array using circular polarization. The rectenna utilized circular microstrip antennas (CMAs) and a bridge rectifier configuration. As Brown's prior experiments, this was another example of a high receiving power application; rectenna input powers from 100 to 10,000 mW were utilized. Within a sub-array configuration, the total number of rectenna elements on the

24

array was 2,304; this gave a peak RF-to-DC efficiency of 64 percent with an input RF power of 2-4 W [19]. McSpadden, Little, et al proposed in 1996 "In-Space Wireless Energy Transmission" [29] where a target for MPT is acquired and maintained. The experiment involved a planar phased array antenna housed on the space shuttle bay that beams to the target rectenna on the free-flying Wake Shield Facility (WSF) with a pilot guide signal beam. The WSF follows behind the shuttle, taking advantage of the vacuum "wake" generated by shuttle movement (which has been shown to be 1,000 times better than the most advanced laboratory vacuum chambers on Earth). This naturally occurring vacuum environment was shown to be useful for epitaxial thin-film materials processing in space [30]. The linearly polarized phased array antenna would transmit 1 kW of power a distance of 100 meters, allowing the rectenna on the WSF to produce a DC output power of 65W [29].

As part of ongoing research related to SPS and MPT, Matsumoto investigated possible nonlinear plasma-wave excitation in the ionosphere caused by high-power microwave beams through two rocket experiments: the Microwave Ionosphere Nonlinear Interaction Experiment (MINIX) and the International Space Year-Microwave Energy Transmission in Space (ISY-METS) [17]. These two experiments provided significant results on non-linear wave interaction in ionospheric plasma caused by microwave power beams, as well as proving that MPT in space is possible. Losses through plasma-wave excitation were shown to be less than 1 percent of total transmitted power [31].

As of 2010, developments in microwave power transmission related to SPS have continued to evolve, particularly in Japan at the Research Institute for Sustainable Humanosphere, Kyoto. Current research for MPT is focused on developing a phased

25

array power transmitter to control beam direction that is highly efficient and low-cost. Cost and efficiency are paramount for the sake of establishing MPT commercial applications, and according to [32], are the reasons more commercial applications of MPT do not currently exist. A transmitting phased array for SPS and MPT is currently being developed at Kyoto University as a part of a government program. The phased array is composed of 256 elements, operating at 5.8 GHz, having an output power of 1.5 kW and a total DC-to-RF conversion efficiency of greater than 40 percent. Additionally, a receiver phased array is being developed with an efficiency of greater than 50 percent and an output power of 0.1 mW for each individual rectenna element. The purposes of advancement are not limited to SPS, they are in part due to the anticipation of future commercial MPT applications, such as ubiquitous power sources for wireless cell phone charging, MPT for wireless power distribution systems in buildings [20], and wireless charging of electric vehicles [32]. However, there are still obstacles to overcome before MPT can be considered for commercial applications. One important issue is frequency regulation in an already crowded spectrum, especially within the ISM band. Another concern, according to [20] is the shortage of effective and economical MPT applications. Most research in the realm of MPT has been single point-to-single point transmission; however there are few recognized advantages to MPT over wired power transmission in this regard.

2.4.3　MPT for Wireless Power Distribution Systems in Buildings

With respect to a single point-to-multiple point configuration, especially with low-power devices, there is much promise for MPT. Devices such as ICs, sensors and RF-IDs that operate within the microwatt range are reasonably applicable in MPT, where a single point source could power many devices at one time. Buildings, being closed area environments, where high power MPT systems can operate within current frequency regulations, provide many opportunities for wireless power transfer. Shinohara, et al, have proposed an indoor wireless power distribution system (WPDS), whereby power is distributed wirelessly using existing building components—for example, deck plates. Within this system, such components are utilized as microwave transmission waveguides; the microwaves propagate within the medium and there is no radiation [20]. The use of existing building components reduces the initial cost of construction for automated buildings. Additionally, rectennas are placed as DC outlets on the floor and can be moved practically anywhere since microwaves exist everywhere within the floor. The proposed system could be useful in an office environment where DC driven "OA" instruments are frequently used, such as computers, fax and copy machines, refrigerators, etc. It has been estimated with WPDS that one DC outlet needs < 50W and within this proposed work a single room has been provided with microwave power >3kW, at an operating frequency of 2.45 GHz. For the purposes of this project, a highly efficient rectenna is designed using Schottky barrier diodes. To achieve a rectification of 100W, a 64-way power divider configuration is used with 256 total diodes. The rectenna has provided 55 percent RF-to-DC conversion efficiency with an input of 100W, at a physical size of 125 mm x 110 mm, x 95mm [20]. Several companies within the United States have recognized the

27

potential of MPT and have taken an active approach to development in this area [33], [34], [35]. MPT applications of this kind display a very promising future in many areas of automation, and could evolve to become a source of immense energy conservation through increased usage efficiency.

Many applications of wireless power transfer with rectennas have utilized a variety of antenna polarization techniques and power density operations. Linear polarization was used for low-power density rectennas in [24], which proved to be useful for transponders in a sensor or communications system in which the interrogation signal also supplies power to the transponder. Additionally, linear polarization was seen in [12] for the purpose of in-space wireless energy transmission. Dual polarized antennas were seen in [25] and [26], useful for low-power signal detection and operation of mechanical actuators. Circularly polarized receiving antennas were employed for the purposes of [19], [36], and [37]. These polarization techniques were shown to be effective for microwave power transmission within SPS and distributed monitoring sensor systems within infrastructure, with efficiencies as high as 78 percent. Low-power density operation was the focus of [13], [14], and [4], and it was proven to be successful within the realm of wireless powering of low-power indoor sensor networks and remote sensors, as well as recycling of ambient microwave energy.

2.5   Rectennas and Remote Wireless Sensing Networks

As previously investigated, diode integrated rectennas have been shown to be useful within many applications of wireless power. However, these devices are instrumental within yet a broader scope of applications—one important application being sensing, monitoring, and communication within remote wireless networks. The spectrum of monitoring and sensing is extensive, including: temperature and humidity sensing, light and laser detection, chemical and biological sensing, sound and vibration detection, and radio/IED/radar detection. Rectennas play a key role within remote sensor networks not only by providing power to the system; they are an essential element to communicating collected information within a sensor network back to a data collection device.

2.5.1   Rectennas and Retrodirective Array Systems

Research on rectenna arrays has continued within this important field, and numerous approaches have been taken to find fitting solutions to current obstacles and to streamlining existing systems. In [38], an adaptive power controllable 5.8 GHz Retrodirective Array System is proposed, which is useful for wireless sensor servers that behave as access points between wireless sensors and remote data collectors. A Retrodirective Array System is described as being able to respond to an incoming signal with a return signal not having prior knowledge of the originating source's location. This "self-beam-steering" capability is effective in numerous remote network applications such as monitoring, data collection, in-space applications, etc. Within the array system is an integrated rectenna and analog switch that controls a battery source. It is able to

29

conserve battery power in idle mode and wake when operation is necessary, thus prolonging its lifetime. An incoming RF signal wakes the system by accumulating power at the input that is converted to DC voltage, thereafter activating a switch and battery. The arriving signal is split between the rectenna and receiver, where the majority of the power is directed to the rectenna. In the absence of an interrogation signal, the switch remains open and the system is off. In [39] a 60 GHz Retrodirective Array System is developed for multimedia sensor server applications. This system streamlines battery efficiency of remote sensors through an incorporated interrogation scheme that uses "wake" and "sleep" commands to turn on/off the system at different times, according to required usage times. When the received power is above 0.013 mW/cm^2, the system powers on and operates as a Retrodirective Array. In addition to streamlining power efficiency, the proposed system uses a microwave frequency of 60 GHz to be compatible with higher data rate requirements, which are often needed in certain remote monitoring applications.

2.5.2   Rectennas for Monitoring and Sensing of Infrastructure

The life span and current conditions of the reinforcement of infrastructures such as buildings, roads, and bridges and is of major concern for public safety in modern times. Developing sensor network technologies can be significantly beneficial in helping assess the continuously changing conditions of infrastructure. For example, miniaturized embedded sensors can monitor steel reinforcement tendons inside the concrete covering of a bridge, and can be deployed during the construction process, as discussed in [37]. It has been shown that detecting cracks or deformations in infrastructures can be achieved

30

through the use of embedded active acoustic wave transducers operating within the ISM frequency band [3]. However, there is a need for an intermediate technology to process and transmit the collected information from these sensors to an appropriate destination, as well as power the embedded devices. A mobile test unit—using an on-board rectenna—has been proposed in [37] as a means to do so. There is also anticipation of future "in-situ" surface-installed supervisory control sensors that will be in the vicinity of such embedded sensors, and these control sensors will perform the function of data transmission and powering. Circularly polarized antennas within the rectenna devices are again recommended as a means of obtaining constant DC voltage regardless of rectenna rotation. In [37], a rectenna featuring a circularly polarized microstrip patch antenna is proposed, which can provide wireless battery powering at 5.5 GHz and data delivery within the 5.15-5.35 GHz WLAN band.

2.5.3 Energy Harvesting and Recycling for Use in Sensor Networks

It is very probable that the future will see a ubiquitous presence of remote sensors, beyond the aforementioned infrastructure applications. Areas such as intelligent office spaces, medical monitoring, surveillance systems, military, construction and manufacturing, and even agriculture will very likely become enveloped with the technology in the coming decades. Along with this expected presence comes the need to efficiently harness and deliver the energy required by low-powered sensor networks. There is much research in the field of energy harvesting and energy recycling utilizing rectenna technology for these purposes.

31

RFID is a popular technology for sensor networks and should continue to be in the future. For the purposes of powering batteryless RFID sensors, a low-profile planar rectenna has been proposed which scavenges ambient RF power from the surroundings and delivers to sensors within a wireless network [40]. The described rectenna technology is integrated with the RFID sensors themselves and operates at 2.4 GHz. A two-stage Dickson zero-bias Schottky rectifier circuit with a miniaturized antenna provides a RF-to-DC conversion efficiency of approximately 54 percent at an input power of 10 dBm. Recycling of ambient microwave energy with broadband rectenna arrays has been described in [4], utilizing low-power density microwave radiation. The purposes of this work are also focused on the wireless powering of industrial sensors within a network structure. A 64-element dual-circularly polarized spiral rectenna array was designed and characterized over a frequency range of 2-18 GHz. Measurement of the rectenna was made with broadside linear polarized radiation at 3 GHz with an incident power density ranging from tens of nW/cm^2 to 0.1 mW/cm^2. Rectification efficiency was seen to reach the 20 percent range for an incident power density of 0.1 mW/cm^2 with arbitrary polarization [4].

2.6   Wireless Passive Surface Acoustic Wave Sensors

Another form of passive technology shown to be useful in the realm of sensing is surface acoustic wave (SAW) technology. By exploiting the piezoelectric effect of the material on which they are fabricated on (quartz, lithium niobate, lanthanum gallium silicate, etc), SAW sensors convert acoustic waves to electronic signals. The conversion is typically achieved through an inter-digital transducer within the device. Much research

32

within the subject of SAWs has been conducted within the past twenty years [41]. Sensing applications related to many areas such as optical, thermal, biological, chemical, and pressure have seen developments.

In particular, passive wireless SAW sensors have shown to be very useful for in-space applications involving structural health monitoring (SHM) of space-vehicles as seen in [42]. In an area where constant close range monitoring of the physical structure of space-vehicles is crucial, passive SAW sensors offer many advantages. Wireless passive SAW sensors offer a solution to many cost, mass, volume, and power constraints within SHM instrumentation on a space-vehicle, and often eliminate the need for heavy wiring and battery requirements associated with wired SHM systems. SAW sensors also operate more robustly within a wider range of extreme temperatures often experienced in an in-space environment.

In addition to in-space vehicular applications, [43] explores the use of SAW sensors in rough environments related to motor vehicles. In such environments, SAW sensors have proven to be useful in providing remote readouts to computers located within the vehicle in severe environments that other types of sensors cannot withstand, for example, within heat, dirt, mechanical vibration, or electromagnetic interference. Interrogable SAW sensors used within a network have also been explored. As seen in [44], a technique to allow multiple sensors to operate simultaneously was developed and demonstrated using a network analyzer and sine pulse interrogation. NASA is continuing to sponsor the research and development of wireless passive SAW sensors due to their inherent environmental robustness and ability to operate well in multi-sensor networks.

33

2.7   Rectennas Using Harmonic Re-Radiation for Sensing Applications

Within many remote wireless network applications, monitoring and sensing is made possible by integrating diodes into low-power wireless devices that operate by modifying and re-radiating a received interrogation signal. In [1] a high efficiency diode doubler—also named a frequency doubling reflectenna (FDR)—is implemented and is shown to be an efficient model for a remote sensor. Within this described work, a modulated form of the second harmonic of a received interrogation signal serves as a return communication signal from the remote sensor within a network. In field application, the return communication signal from a remote sensor may contain quantified information with respect to the device's local environment. The device described in [2] is intended for sensing applications and utilizes frequency discrimination to enhance the ability of an interrogating transceiver—base station—to detect a signal of very low amplitude. Through the employment of a diode, harmonic forms of the incoming interrogation signal at 1.3 GHz are produced and a single harmonic at 2.6 GHz is retransmitted. The topology of the FDR is presented in Figure 2.4.
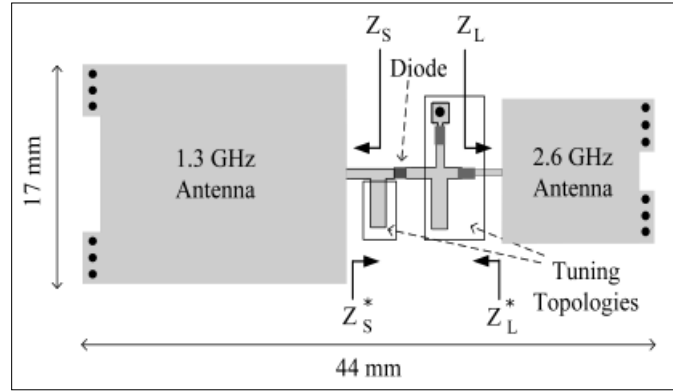
Figure 2.4: Layout of Frequency Doubling Reflectenna transponder [2]

A GaAs Schottky diode is chosen for the doubling element, as this type of diode
has proven to perform with high conversion efficiencies at microwave frequencies. The
transponder also consists of two quarter-wavelength, shorted microstrip patch antennas,
and matching stubs to provide a conjugate match to the diode. The matching elements
associated with the antennas provide a source impedance that is very close to the complex
conjugate of the input impedance to the diode, thus minimizing conversion loss and
maximizing device efficiency. It is reported in [2] that doubler conversion efficiency
$\left(n_n = \dfrac{P_{out}}{P_{in}} \right)$ of 1% was achieved at -30 dBm input power level. As previously discussed, a
bias can improve conversion efficiency and provide modulation characteristics, however
for the described work, in the interest of maintaining a simple design, the bias has been
neglected. Figure 2.5 shows relative measured power output levels from the tag according
the respective frequencies of operation. This will be further discussed and comparisons
will be made in Chapter 3, with a description of how the FDR was incorporated into the
work of this thesis. Figure 2.5 shows the varying output power (at $2f_0$) versus input power

35

(at f_0) three different fabricated FDRs. The FDR labeled 'FDR1' was the device utilized in this work, which is closest to 1.291 GHz operating frequency. Figure 2.6 shows changing conversion gain and DC current over a varied input power to the FDR of 0 to -50 dBm. The proposed harmonic re-radiating rectenna device could be useful for quasi-optical applications, energy scavenging, and monitoring and sensing [2].
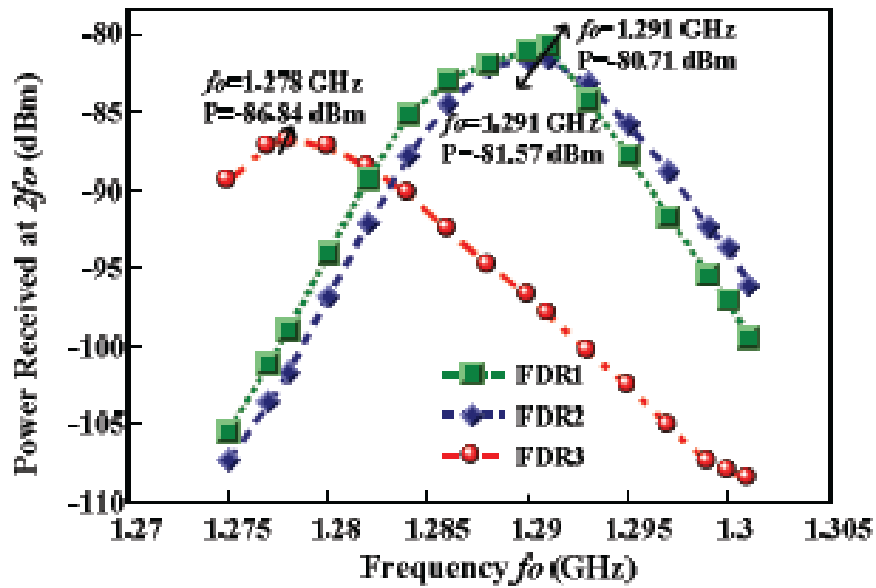
Figure 2.5: Received power vs. frequency for 3 FDR devices
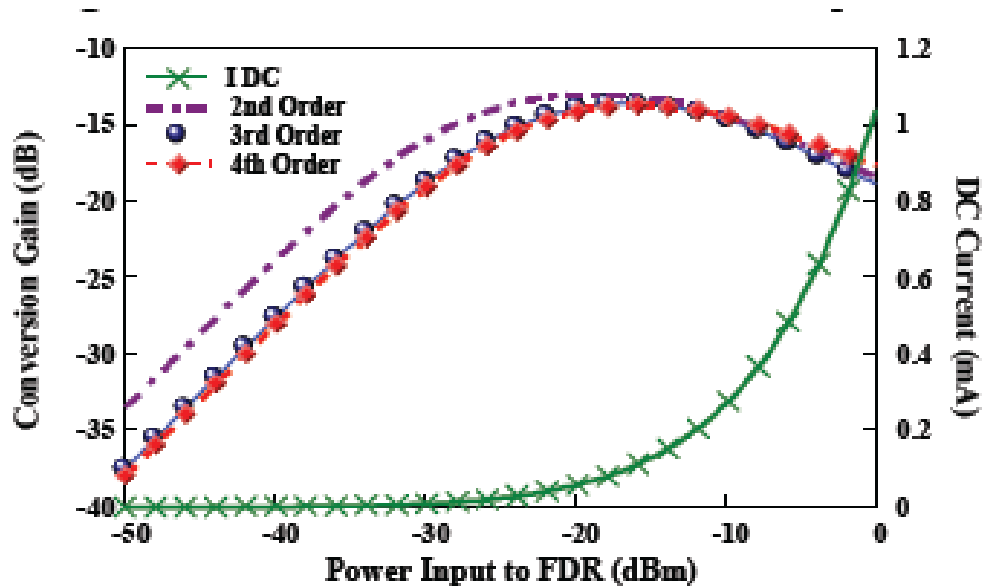
Figure 2.6: Conversion gain vs. frequency for 3 FDR devices

2.8   Conclusions

In summary, a rectenna was described as a diode and antenna integrated device, useful in a broad spectrum of low- and high-power applications. A background of diode theory was presented, as the Schottky diode is a key component to a rectenna device. Rectenna and rectenna array application technologies have been explored, from wireless microwave power transfer to remote wireless sensor networks. Much of the ongoing research within rectenna technologies exhibits promise for continued improvements in communications, safety, and energy conservation.

37

CHAPTER 3

REMOTE INTERROGATION SYSTEMS WITH HARMONIC RE-RADIATION

3.1   Introduction

Although the concept of microwave detection has existed since WWII, when radar was the first major application of microwave technology, significant advances still continue to be made within the field [11]. Such advances are especially noticeable within the realm of integrated devices for sensor communication networks. The issues of cost, size, and efficiency continue to be addressed through the developments of higher-efficiency miniaturized devices, such as [45]. For particular sensing networks involving remote communication devices, enhancements in size and efficiency of devices at times is not sufficient for detectability of low-strength signals. To assist with the task of measuring low-strength signals, lock-in amplifiers have been employed. The goal of the work described within this chapter was to incorporate the harmonic re-radiator from [2]—which possessed significant size and operating efficiencies—into a unique configuration termed the "Remote Lock-In Amplifier" (RLIA). The RLIA approach utilizes lock-in amplification in a remote connection scheme that separates the heavy electronics from the sensor. The interrogation equipment that require more power for operation are located at a mobile base-station platform, allowing the sensor to operate with "zero" power conditions.

38

3.2   Introduction to Lock-In Amplifiers

One notable contributor to the evolution of signal detection is the lock-in amplifier. Lock-in amplifiers are devices used to detect extremely small AC signals reaching as low as -100 dBm or more. It is not uncommon for lock-in amplifiers to operate with sensitivities well into the nano-volt range, where signals may be detected in the presence of an excessive amount of noise, which would otherwise obscure a signal. These devices have proven to be useful in many different measurement applications including: complex impedance measurement for nano-wire gas sensing [6], accurate measurement of modulated-scattered electric fields [7], and measurement of open-path scattered light from fine particles such as diesel particulate emissions [8].

The technique employed by lock-in amplifiers to perform such tasks is referred to as "phase-sensitive detection" and entails singling out a signal component at a specific reference frequency. Noise signals at all other frequencies are rejected by the lock-in amplifier and thus do not contribute to the measurement. According to Fourier's theorem, representation of a signal in the frequency domain is possible as a sum of many sine waves occurring at different amplitudes, frequencies and phases [46]. Time domain representation of signals, as in the case of normal oscilloscopes, often does not bear enough information about the various frequencies that make up a signal unless it is a clean sine wave [9]. However, a lock-in amplifier avoids this by way of multiplying each component of the input signal with a pure sine wave at the reference frequency contemporaneously. In general, unless two frequencies are identical, the average of the product of the two sine waves will be zero. The multiplication done by the lock-in amplifier produces a DC signal proportional to the component of the received signal that

39

has a frequency exactly locked to the reference frequency. Following the multiplication that occurs, a low-pass filter removes the components at all other frequencies other than the reference frequency.

3.2.1   Phase-Sensitive Detection

The process of Phase-Sensitive Detection utilized by lock-in amplifiers essentially deciphers an experimental signal from noise. The measurements performed by lock-in amplifiers require the input of a reference frequency. The experiment being performed is stimulated at this fixed reference frequency via either a function generator or oscillator, and the lock-in amplifier detects the output response of the experiment, which will contain the desired signal information at the reference frequency [9]. All other frequencies are unnoticeable to the lock-in amplifier. As shown in Figure 3.1 the reference signal, provided by the function generator, is a square wave. This signal is directed into the lock-in amplifier so as to provide the reference according to the frequency it should be "looking at" from the incoming experimental signal.
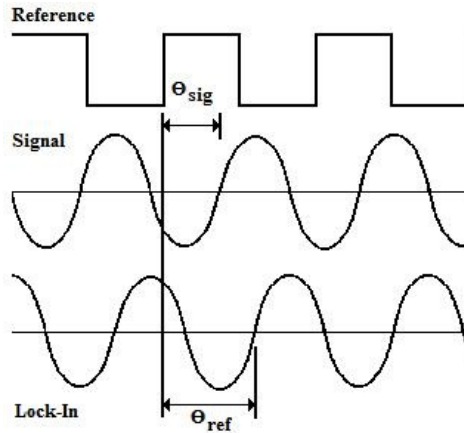
Figure 3.1: Phase sensitive detection performed by a lock-in amplifier

Lock-in amplifiers employ a Phase-Locked-Loop (PLL) fixed on the external reference, which in turn generates an internal reference signal. Figure 3.1 shows the external reference square wave, the experimental signal, and the internal reference signal of the lock-in amplifier. According to [9], the internal reference signal is defined as:

$$V_{lock-in} = sin(\omega_{lock-in}t + \theta_{lock-in}) \qquad (3.1)$$

The experimental signal is amplified and multiplied by the reference signal through a phase-sensitive detector (PSD) or multiplier. The output of the PSD provides a signal that is equal to the product of the two sine waves, as shown below [9]:

41

$$V_{PSD} = V_{signal}V_{lock-in}\, sin(\omega_{ref}t + \theta_{signal})\, sin(\omega_{lock-in}t + \theta_{ref}) \qquad (3.2)$$

thus,

$$
\begin{aligned}
= {}^{1}\!/_{2}\, V_{signal}V_{lock-in}\, &\left(\cos(\omega_{ref} - \omega_{lock-in})t + \theta_{signal} - \theta_{ref}\right) \\
&- {}^{1}\!/_{2}\, V_{signal}V_{lock-in}\, \left(cos(\omega_{ref} + \omega_{lock-in})t + \theta_{signal} - \theta_{ref}\right) \quad (3.3)
\end{aligned}
$$

The output of the PSD consists of two AC signals, one existing at the sum frequency of $(\omega_{ref} + \omega_{lock-in})$, and the other at the difference frequency of $(\omega_{ref} - \omega_{lock-in})$. When the output of the PSD is subsequently passed through a low-pass filter, AC signals will be removed. If $\omega_{ref} = \omega_{lock-in}$ the difference frequency will be a DC signal proportional to the signal amplitude and will be equal to [9]:

$$V_{PSD} = {}^{1}\!/_{2}\, V_{signal}V_{lock-in}\, cos(\theta_{signal} - \theta_{ref}) \qquad (3.4)$$

With traditional analog lock-in amplifiers, the reference and experimental signals are analog voltage signals. The two are multiplied in an analog multiplier and passed through at least one stage of RC filters. The lock-in amplifier could not successfully detect an experimental signal at the reference frequency without the use of narrow band detection. Since the input to the lock-in amplifier consists of signal plus noise, it is important for it to have a low-pass filter with a very narrow bandwidth. The PSD and

42

low-pass filter are limited to detecting signals very close to the reference frequency. This causes noise signals that occur at frequencies far from the reference to be attenuated and is a key concept in the operation of the lock-in amplifier [9]. If noise signals occurring at frequencies very close to the reference frequency exist, the output of the PSD will observe very low frequency AC signals. The strength of these leaked noise signals depends on the roll-off and bandwidth of the low-pass filter. The bandwidth of the low-pass filter ultimately determines the bandwidth of detection for the lock-in amplifier; a wider bandwidth will allow some of these noise signals to pass and a smaller bandwidth will attenuate the noise signals close to the reference. The experimental signal (the only signal occurring at the exact reference frequency) will be unaffected by the low-pass filter, as it will be a true DC signal, and this is the signal of interest for measuring [9].

Another necessary component of the lock-in amplifier is the PLL. For proper measurement of the experimental signal, it is required that the reference and the experimental frequencies be equal and have equal phases unchanging with time. A change in the two phases will cause $cos(\theta_{signal} - \theta_{ref})$ to change, and subsequently V_{PSD} will not be a DC signal. Therefore, the lock-in amplifier utilizes a PLL to lock the internal reference oscillator to the external reference, providing a consistent reference sine wave at ω_{ref} with a fixed phase shift of θ_{ref}. This feature ensures that a change in the external reference frequency will not disturb the measurements [9].

43

3.3   Detector and Lock-In Amplifier Characterization

In Chapter Two a discussion of the characteristics of the Schottky barrier diode was presented. Another important characteristic of a diode detector, particularly when an application requires measurement of extremely low-power signals, is Tangential Sensitivity (TSS). According to [47], the TSS of a diode detector is the lowest signal power level for which the detector will have a specified signal-to-noise ratio at its output. Measurements of TSS along with voltage sensitivity are useful in radiometer applications. As seen in [48], TSS measurements can be performed to estimate noise equivalent power (NEP) of the detector itself. In this TSS measurement procedure, input power levels are set such that the value where the noise peaks without an RF signal equals the lowest noise with an RF signal. Then using an oscilloscope and video amplifier the actual value of TSS can be measured. This type of procedure could enhance voltage sensitivity of a measurement system where the absolute highest sensitivity values are critical.

In characterization phase for the coaxial detector and lock-in amplifier, various testing equipment was incorporated into a bench-top configuration and measurements were performed. This was a necessary step in the progression of the RLIA concept since future tests would require a reference for measurement verification purposes. The block diagram in Figure 3.2 shows the equipment used in the configuration: Standard Research Systems Model SR530 lock-in amplifier, Narda Zero Bias Crystal detector Model 4503-01, variable attenuator, standard signal generator, and standard function generator. The documented measurements constituted the effective sensitivity of the detector and verified proper function of the lock-in amplifier. A voltage sensitivity curve was

44

constructed from the results, and the Narda detector data sheet was used as a reference to verify the sensitivity measurements (Appendix A).
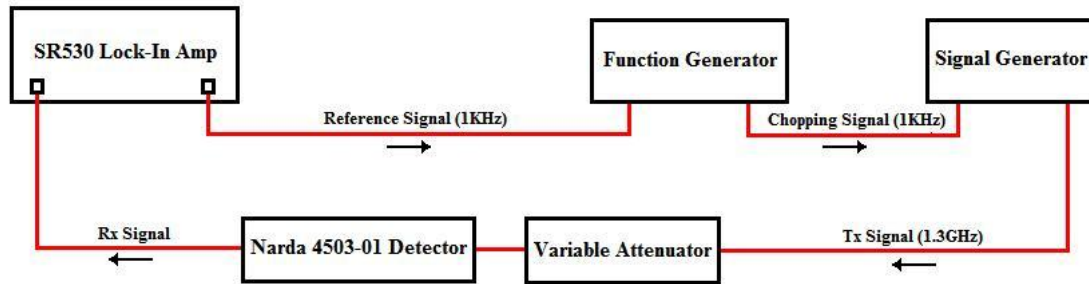
Figure 3.2: Block diagram of detector characterization Using Lock-In Amplifier

The role of the signal generator in the bench-top configuration is to provide the fundamental signal source (1.3 GHz) to the detector through a variable attenuator, which is then fed to the lock-in amplifier. The function generator provides the reference signal for the lock-in amplifier (1 kHz square wave, 100 mV) as well as the chopping frequency (1 kHz sine wave, 100 mV), which is the imparted modulation onto the source signal. Without both the reference signal and the modulating chopping frequency, the lock-in amplifier is unable to perform its function. Between the signal generator and the detector is the variable attenuator, emulating channel loss. The presence of the variable attenuator in the configuration provides a way to consistently reduce the signal power level, imitating the effects of free space path loss, while keeping the source at a maximum signal output level.

In order to have a reliable test environment, the performance of the standard equipment was verified. Before constructing the detector/lock-in characterization set-up,

45

initial measurements were performed on the signal generator using a power meter to verify the output power and obtain calibrated signal values. The signal generator was programmed to give a continuous wave output of 1.3 GHz at an amplitude of 0 dBm, then the output was measured by the power meter with the variable attenuator attached. Calibration measurements were performed in order to establish a 0 dBm reference point including losses from cables and the variable attenuator. This reference point was achieved with a 2.0 dBm output from the signal generator. The coaxial detector was then introduced into the circuit at the output of the variable attenuator, in series with a multimeter (which was later replaced by the lock-in amplifier). With this configuration it was possible to compare the dc voltage output of the detector to the known calibrated power input to the detector. Attenuation was decreased in increments of 1dBm and the output voltages (mV) from the detector were recorded as seen in Figure 3.3 (Table I, Appendix A).
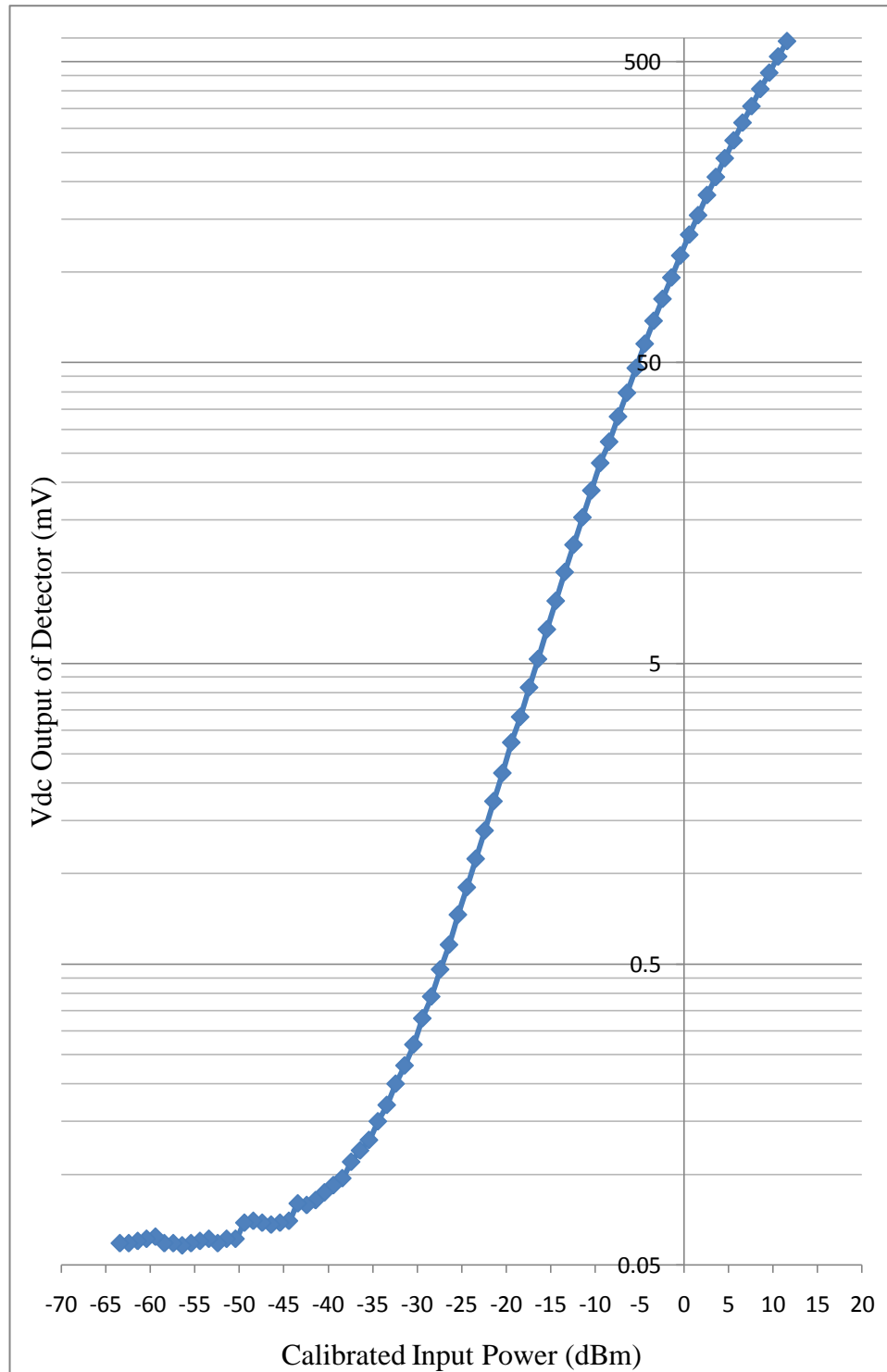
Figure 3.3: Measured voltage sensitivity of Narda detector (Model 4503-01) using Lock-In Amplifier

47

The signal source was set to its maximum power output of 14.5 dBm (a calibrated power output of 11.58 dBm accounting for losses) and the variable attenuator was increased in 1 dB steps. The measured signal voltage at the output of the detector vs. input power is shown in Figure 3.3. Stable measurements were acquired from 11.58 dBm to ~ -50 dBm, at which point fluctuations in voltage output were seen, indicating the TSS threshold for the detector.

3.4   Background Work on Sensor Node Harmonic Repeaters—1st Generation Transponder

As previously introduced in Chapter Two, a high-efficiency frequency doubling transponder was developed for low-power sensing applications [2]. Using the principles of frequency multiplication, this device receives an interrogation signal at 1.3 GHz and retransmits the harmonic at 2.6 GHz. This transponder is used to verify the RLIA concept and is considered the 1st generation device. The printed circuit board design consists of two quarter-wavelength patch antennas (1.3 GHz and 2.6 GHz) and a diode-based doubler. Each antenna is operated near its respective resonant frequency, where the impedance changes rapidly as a function of frequency. By this and conjugate-matched conditions on both sides of the multiplier (Figure 3.4), a bandwidth of less than 0.5%, is achieved. In order to provide an intrinsic match to the diode doubler impedance under very small-signal conditions, the transponder antennas are designed such that the impedance of the receive patch antenna is ~34 + j305 Ω at 1.3 GHz and the impedance of the transmit patch antenna is ~40 – j355 Ω at 2.6 GHz. Expected and measured conversion gain vs. input power for the 1st generation transponder at 1.3 GHz is shown in

48

Figure 3.5. When properly functioning, the 1st generation transponder will have a conversion gain of approximately -20 dB at an input power level of -30 dBm, and approximately -15 dB at an input power level of -20 dBm (Figure 3.6). Peak multiplier efficiency of ~2% at -30 dBm input power was seen as in the figure, and this was achieved over a frequency sweep of 1.27 GHz to 1.305 GHz. Efficiency is also seen to remain relatively flat over a 30-40 dB input power range [2].
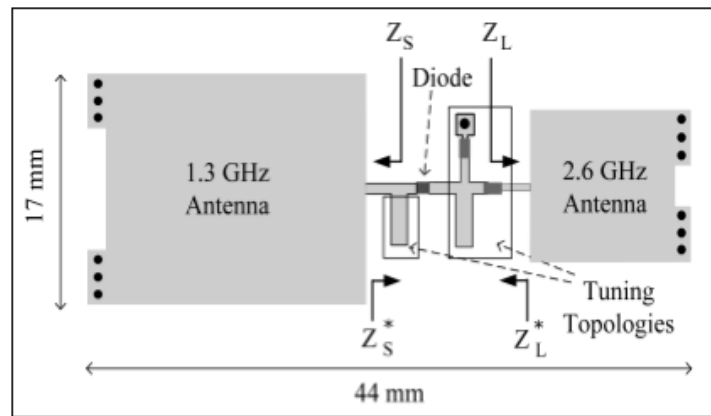
Figure 3.4: 1st generation transponder layout: Z_S and Z_L are the input and output impedances of the diode. Z_S* and Z_L* are the source antenna input impedance and load antenna input impedance, respectively [2].
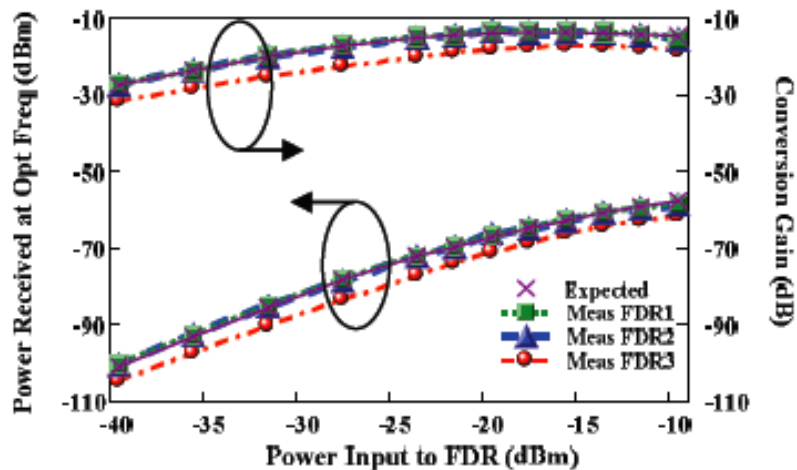
Figure 3.5: 1st generation transponder expected and measured conversion gain vs. input power at 1.3 GHz.

49
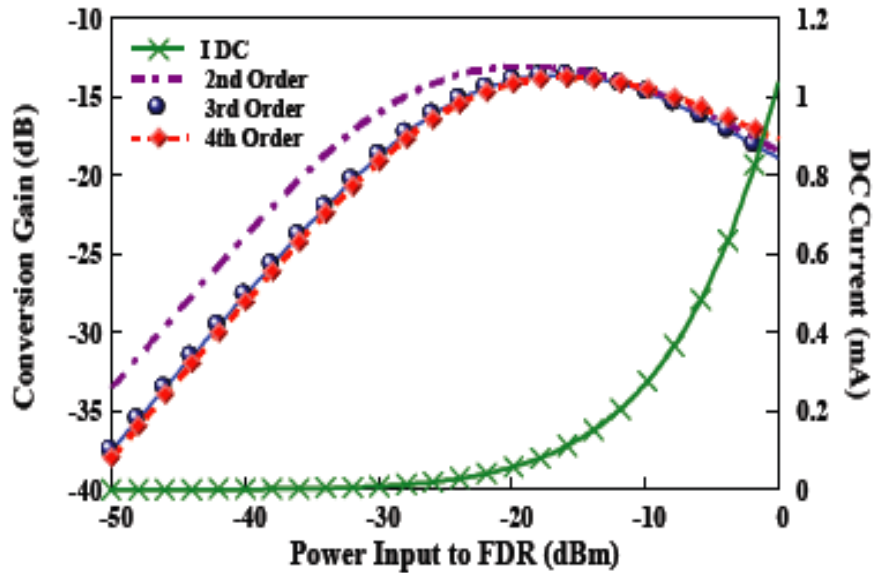
Figure 3.6: 1st generation transponder conversion gain vs. input power

As cited in Chapter Two, other diode-integrated rectenna designs have shown greater RF-to-DC conversion efficiencies, however, this is in the case of much higher transmit powers (wireless power transfer for example).

3.5   1st Generation Transponder within RLIA System

The following section presents the configuration of the 1st generation transponder within the RLIA system, measurements and analysis. The first major test involving the full RLIA system focused on demonstrating the capability to effectively communicate with the low-power remote transponder and to verify system link budgets. This name can be used due to the fact that the device itself requires no additional power to operate, other than that carried within the radio signal itself. This is an important feature for many remote-sensing schemes where long life with minimal maintenance is a concern. The 1st

50

generation transponder demonstrated proof of concept by processing relevant information under "zero" power operating conditions. The full RLIA test set-up was configured so that when an interrogation signal is transmitted at a particular frequency, a return signal is received from the transponder at double the frequency with the sensor signal modulated onto the carrier. The full test configuration was performed with a distance of 1.5 meters and is shown in Figure 3.7. The transmitter block is comprised of a 1.3 GHz signal source, a function generator that modulates the 1.3 GHz signal, and a transmit antenna with a gain of 5.05 dBi. The function generator provides a chopping frequency (sine wave form at a frequency of 1 kHz with amplitude of $100mV_{pp}$) that is imparted onto the transmitted signal. The signal arriving to the receiver block may be very weak or may be accompanied by the presence of an overwhelming amount of noise; therefore the chopping frequency will assist the lock-in amplifier in locating the signal components which contain the desired information.

The receiver block consists of the necessary components to properly filter and coherently demodulate the retransmitted signal from the transponder. It is comprised of a receive antenna with a gain of 7.08 dBi, a variable attenuator (to incrementally reduce signal strength at a constant rate), filter and amplification stages, a diode detector and a lock-in amplifier (Figure 3.7).
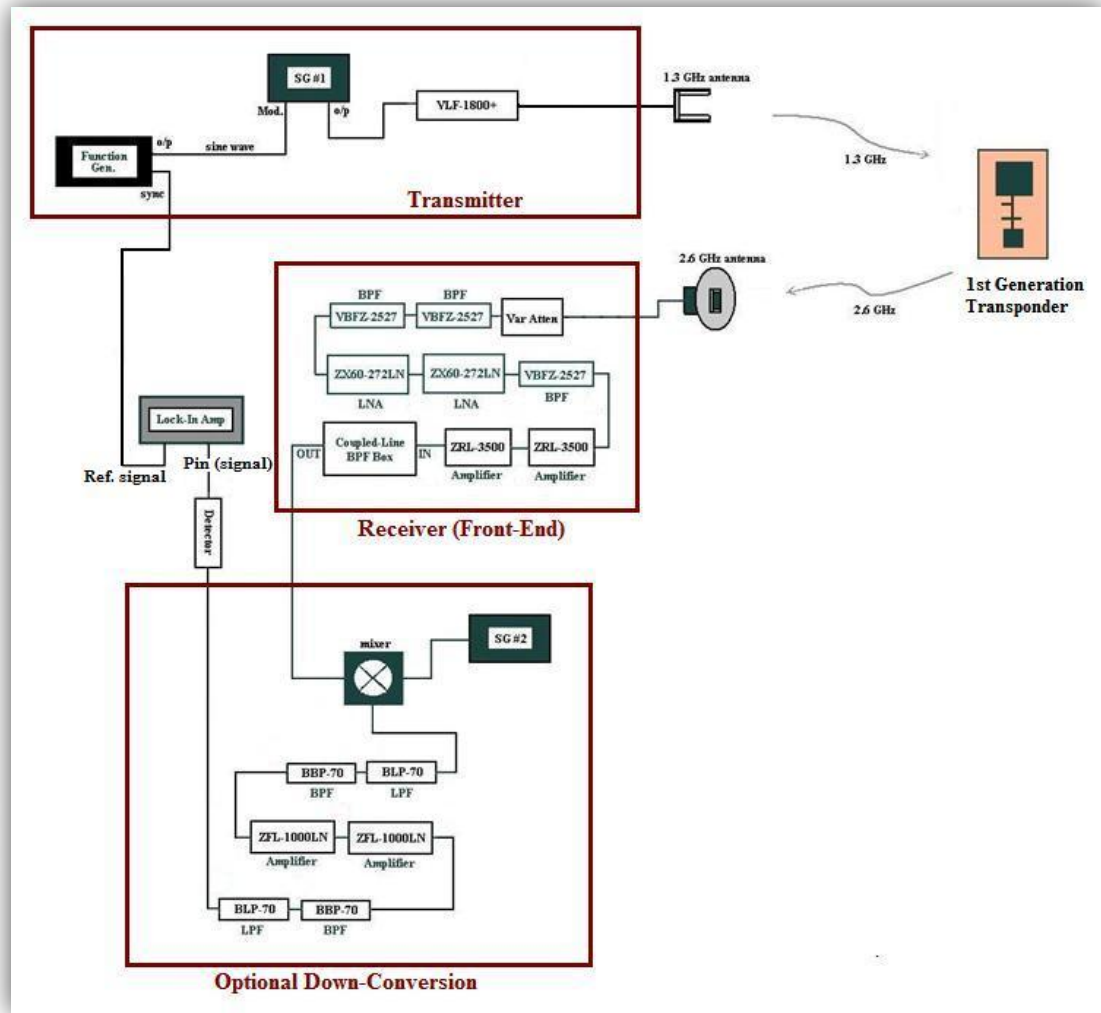
Figure 3.7: Block diagram of full Remote Lock-In Amplifier interrogation system

As aforementioned, coherent demodulation with a chopping and reference frequency is an intrinsic feature that is key to the function of the lock-in amplifier. However, when a detector is introduced and used concomitantly with the lock-in, it is important that the signal reaching the input of the detector be free of undesired interference signals. Since the diode detector outputs a particular DC voltage that is directly proportional to its input power, ideally the input signal to the detector should be solely comprised of the desired information signal. If interference signals (for example ambient signals from WLAN, cellular, microwave ovens, etc.) at significant power levels are allowed to pass through the system and impinge on the detector, inaccurate voltage readings at the output of the detector will result. In light of this, sufficient filtering is crucial—including a possible down-conversion stage—to produce a signal that is free of interference.

The RLIA system is equipped with filters on both transmit and receive blocks and a down-conversion stage yielding an intermediate frequency of ~60 MHz. The down-conversion stage facilitates removal of strong interference signals within the 1.8 to 2.8 GHz band. End-to-end interrogator receiver gain—excluding the antenna—is 75 dB. Link budgets based upon the configuration in Figure 3.7 are listed in Tables 3.1 and 3.2. The difference between the two budgets is the interrogator transmitted power, which is 5.00 dBm and -6.02 dBm respectively. In the budget in Table 3.1(a), the transmitted power at 1.3 GHz is 3.16 mW, which yields an input power of -29.19 dBm to the transponder. At this input power level the harmonic transceiver conversion efficiency is approximately -20 dB. The budget in Table 3.1(b) consists of a transmit power, input power to the transponder, and harmonic conversion efficiency of 0.25 mW, -40.21 dBm, and -30 dB

53

respectively. In the first part of testing the RLIA configuration, a spectrum analyzer was employed; therefore a system bandwidth of 10 kHz is reported in both budgets that correspond to spectrum analyzer settings. Measurements were conducted in an open lab environment and a comparison between calculated and measured output power is given in the bottom two lines of each budget table. As seen in the tables, for transmit powers of 3.16 mW and 0.25 mW the difference in measured and calculated output powers is 1.12 dB and 4.27 dB respectively. These differences could be attributed to additional multipath occurring during experimentation or small interference signals leaking into the system.

Table 3.1 (a) Link budgets for RLIA system at 3.16 mW and (b) 0.25 mW transmit powers respectively

(a)

Interrogator Transmit Frequency	1.30	GHz
Interrogator Transmitter Power	**0.00316**	W
	(5.00)	(dBm)
Loss to Interrogator Transmit Antenna	1.00	dB
Interrogator Transmit Antenna Gain	5.048	dB
Distance to Senor Node	1.50	m
Transmit Spreading Loss	-38.24	dB
Power Received by Sensor	-29.19	dBm
Sensor Receive Antenna Gain	0	dB
Doubler Conversion Loss	-20.00	dB
Sensor Transmit Antenna Gain	0	dB
Re-Transmitted Frequency	2.60	GHz
Distance to Interrogation Node	1.50	m
Re-Transmitted Spreading Loss	-44.26	dB
Interrogator Receive Antenna Gain	7.075	dB
Power Received by Interrogator Node	2303	fW
	(-86.38)	(dBm)
Noise Power Density (kT)	-173.83	dBm/Hz
Interrogator System Bandwidth	10.00	kHz
Interrogator Noise Figure	3.00	dB
Interrogator Noise Floor	-130.83	dBm
Signal to Noise Ratio (SNR)	44.45	dB
Interrogator Receiver Gain	75.00	dB
Power to Detector	-11.38	dBm
Measured Value	-12.50	dBm

(b)

Interrogator Transmit Frequency	1.30	GHz
Interrogator Transmitter Power	**0.00025**	W
	(-6.02)	(dBm)
Loss to Interrogator Transmit Antenna	1.00	dB
Interrogator Transmit Antenna Gain	5.048	dB
Distance to Senor Node	1.50	m
Transmit Spreading Loss	-38.24	dB
Power Received by Sensor	-40.21	dBm
Sensor Receive Antenna Gain	0	dB
Doubler Conversion Loss	-30.00	dB
Sensor Transmit Antenna Gain	0	dB
Re-Transmitted Frequency	2.60	GHz
Distance to Interrogation Node	1.50	m
Re-Transmitted Spreading Loss	-44.26	dB
Interrogator Receive Antenna Gain	7.075	dB
Power Received by Interrogator Node	3.573	fW
	(-114.47)	(dBm)
Noise Power Density (kT)	-173.83	dBm/Hz
Interrogator System Bandwidth	10.00	kHz
Interrogator Noise Figure	3.00	dB
Interrogator Noise Floor	-130.83	dBm
Signal to Noise Ratio (SNR)	16.36	dB
Interrogator Receiver Gain	75.00	dB
Power to Detector	-39.47	dBm
Measured Value	-35.20	dBm

54

The second test portion of the RLIA system involved using both a spectrum analyzer and a lock-in amplifier to detect the received signal measured over a swept transmit power range. For these results the distance from the interrogator to the sensor node was again 1.5 m. Figure 3.8(a) shows the results using a spectrum analyzer, where a minimum detectable power of ~ -55 dBm is demonstrated. To verify the output system noise floor, first the interrogator noise floor was calculated according to kTB, where k is Boltzmann's constant (k = 1.380 x 10^{-23} J/ °K), T is temperature in degrees kelvin (k = 0.599), and B is the bandwidth of the system, which is taken to be the bandwidth of the spectrum analyzer (B = 10 MHz). It is then possible to take the interrogator noise floor value from Tables 3.1(a) and (b) (-130.83 dBm) and add the receiver block gain of 75 dB, arriving at a value of -55.83 dBm. Figure 3.8(b) shows the measured results of testing with a lock-in amplifier in place of the coaxial diode detector and signal analyzer combination. In this testing configuration, minimum detectable signal levels were seen approximately 5 dB below the configuration in Figure 3.8(a). It can be deduced that the detectable signal using the lock-in amplifier is at least 5 dB into the system noise floor, since conversion efficiency of the harmonic transceiver decreases at least linearly with input power, as seen in Figure 3.6.

55
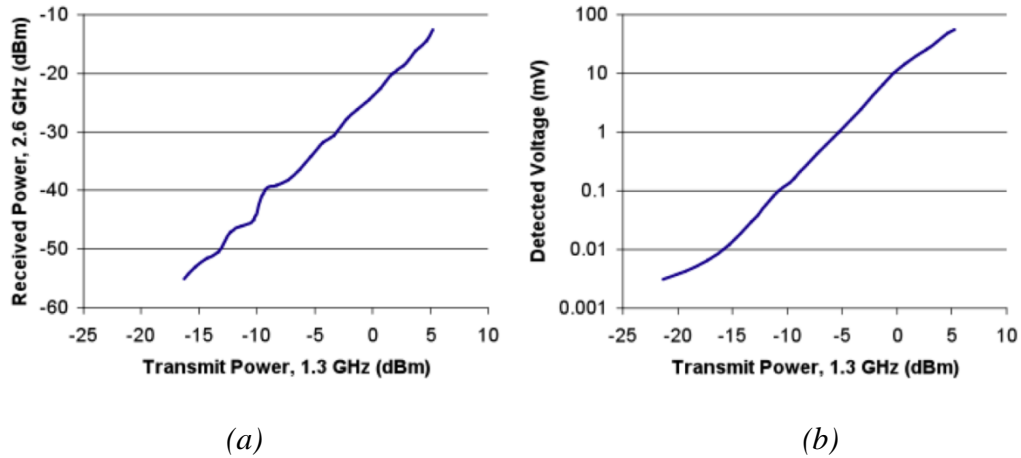
Figure 3.8: (a) Measured performance of the system at an interrogator-to-sensor distance of 1.5 m using a spectrum analyzer; (b) lock-in amplifier

3.6   Design of 2nd Generation Transponder

As the RLIA scheme is further developed, a new version of the transponder is introduced. The existing zero-bias transponder is modified to include a DC bias line with a series inductor and shunt capacitor to block any RF leakage. An applied bias voltage to the diode will directly change the impedance match between the receiving 1.3 GHz antenna and the doubler causing a change in conversion loss. This change in conversion loss induces an amplitude modulating effect on the retransmission of the signal from the transponder. The 2nd generation transponder as seen in Figure 3.9 was fabricated on Taconic, 60 mil (Er=6.15) copper substrate and utilizes the shown Coilcraft inductors (0402) and Johanson capacitors (0402).

56
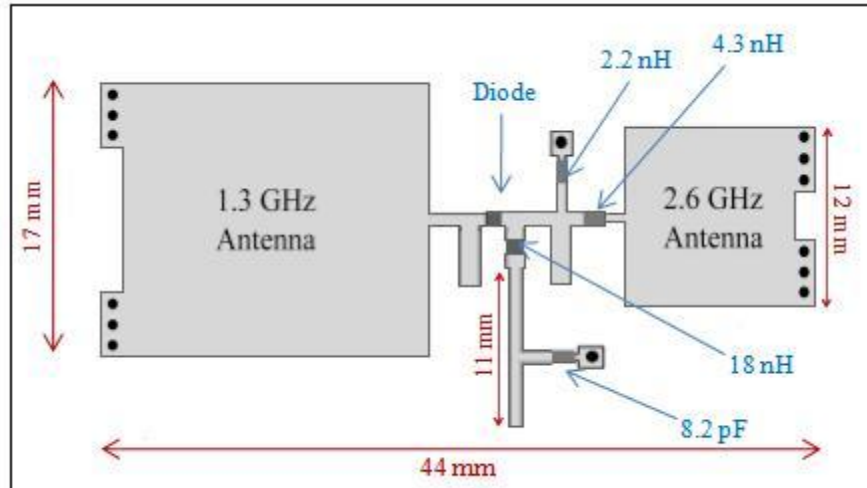
Figure 3.9: Layout of 2nd generation transponder

Referring to Figure 3.6, as input power to the transponder drops below -30 dBm,

conversion efficiency subsequently drops and the same occurs when input power to the

transponder reaches above -20 dBm. Simply increasing the power level of the transmit

signal does not convert to a stronger retransmitted signal from the transponder.

Conclusively, the maximum power the transponder is able to retransmit back to the

receiver is approximately -40 dBm (-20 dBm – 20 dB [conversion loss]). With the best

possible conversion efficiency in mind, testing of the 2nd generation transponder was

performed with an incident power to the transponder within the range of -20 dBm to -30

dBm. In determining the appropriate power level required from the signal generator to

result in an incident power level to the transponder within this range, the proper distance

between the 1.3 GHz antenna and the transponder needed to be calculated. To achieve a

transponder input power within the range of -20 to -30 dBm it was necessary to fix the

source at its maximum level of 14.5 dBm. A link budget of the testing configuration of

the 2nd generation transponder can be seen in Figure 3.10 (Table II, Appendix A). The

free space path loss computation method was used to determine that a transmitted signal of ~12 dBm at a distance of 4 feet would yield an incident input power to the transponder at 1.3 GHz within the optimal range. The receive antenna gain of the transponder itself is 0 dB, therefore the receive power of the transponder is -24.3 dBm, as seen in Figure 3.10.
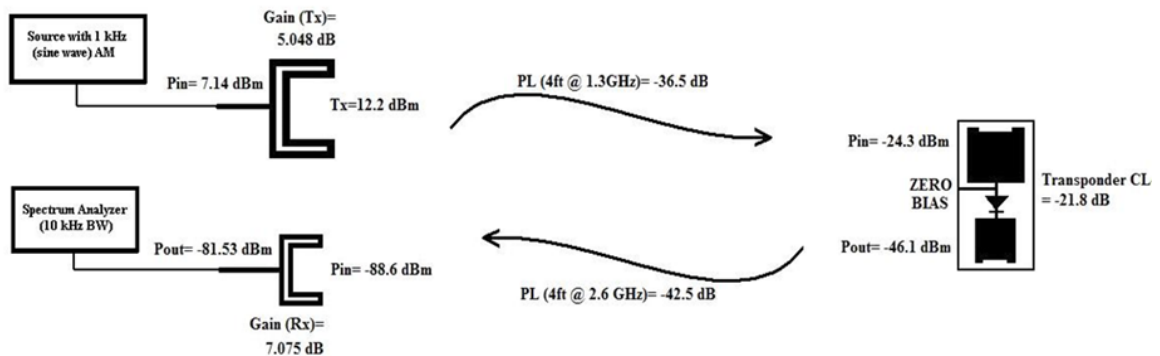
Figure 3.10: 2nd generation transponder testing configuration

In characterizing the transponder, the first test was to identify the optimal transmit frequency, which would translate to the highest output power and conversion efficiency from the device. The source amplitude was kept at a constant 12.2 dBm, and frequency was swept from 1265 to 1315 MHz. The transponder bias was set to a fixed value of 0 V. Measurement results are shown in Figures 3.11 and 3.12, where it can be seen that optimal transmit frequencies and conversion efficiencies occur at 1275 MHz and 1300 MHz.

58
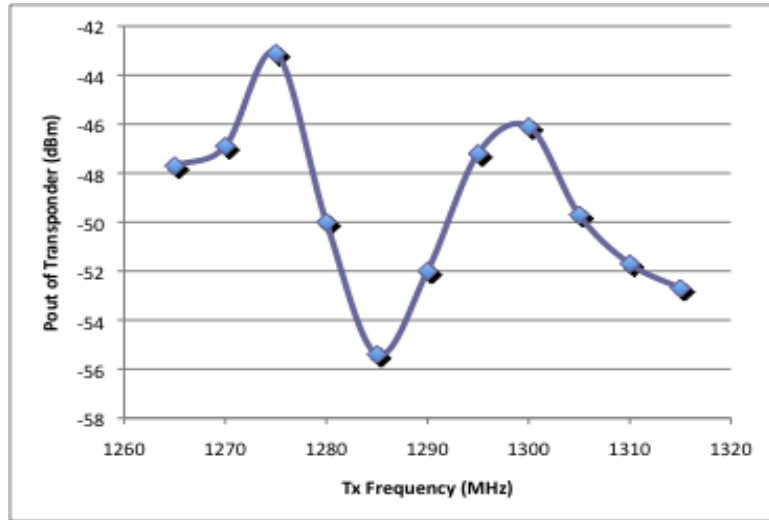
Figure 3.11: P$_{out}$ of transponder at 0 V bias over frequency sweep
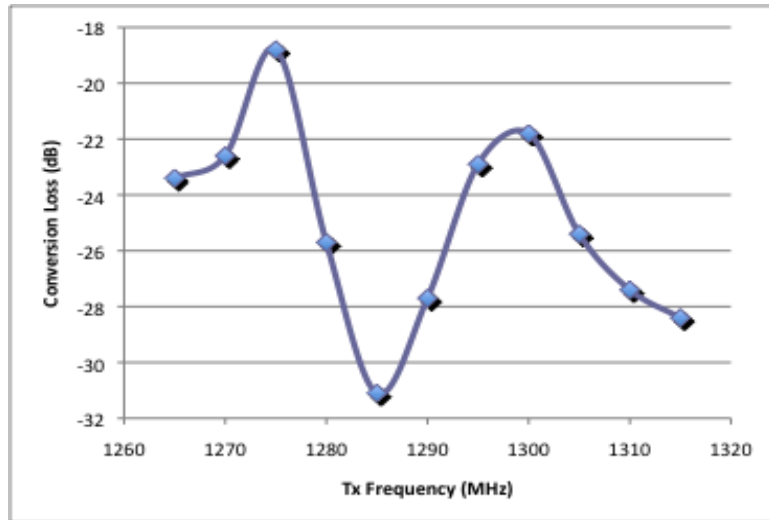
Figure 3.12: Conversion loss of transponder at 0 V bias over frequency sweep

59

Referring to Figures 3.6 and 3.12 and comparing the 1st and 2nd generation transponders, it can be observed that both devices exhibit similar conversion loss behavior at input powers around -24 dBm. The next test in the characterization of the 2nd generation transponder involved fixing the bias and input power level and sweeping the frequency to find the peak retransmitted signal power level, as was done in the previous test; however, in this test the bias voltage was fixed at +/- 0.05 V and then at +/- 0.15 V. The results of this test determined whether a change in bias voltage would cause a shift in frequency. This information is critical in the case of employing a frequency diversity scheme for interrogating sensors in the field. It is imperative to know the exact spectral spacing required for two consecutive sensors to operate without interfering with each other. If a change in bias voltage did in fact cause a shift in frequency, this would cause a single transponder to experience a shifting peak; and without knowing the amount of frequency shift for a single sensor, proper spectral spacing may not be obtained. The consequence of this being that when interrogation is in progress, it would be impossible to determine if a retransmitted signal is being produced by one single transponder, or if another transponder close in frequency is actually producing the signal. As in the former test, the transmit frequency was swept from 1265 to 1315 MHz in steps of 5 MHz. Input power was fixed at the maximum 12.2 dBm to achieve a -24.3 dBm input level and, as seen in Figures 3.13 and 3.14, P$_{out}$ of the transponder is provided according to the respective frequencies.

60
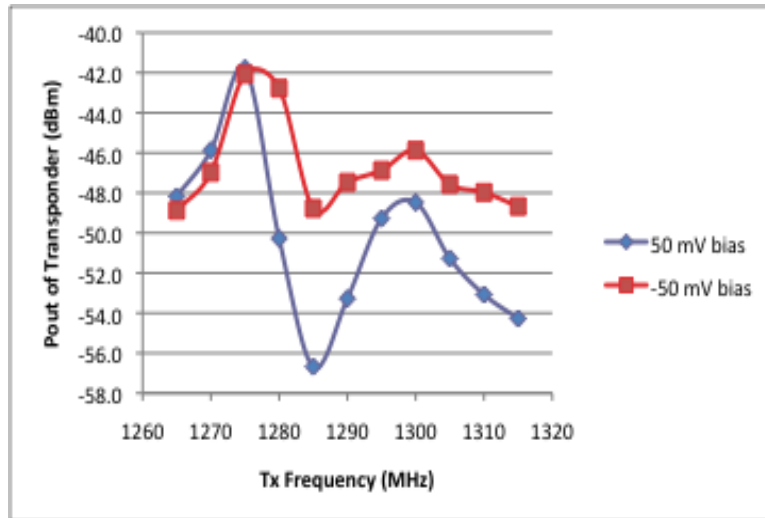
Figure 3.13: P_{out} of transponder at +/- 0.05 V bias over frequency sweep
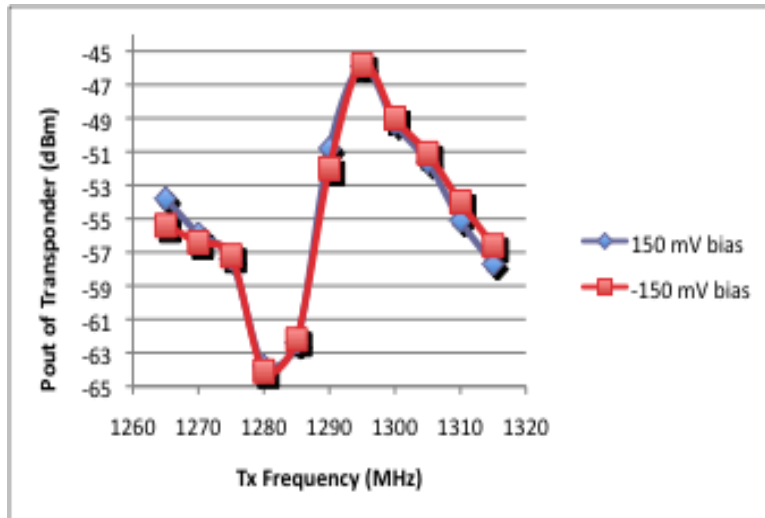
Figure 3.14: P_{out} of transponder at +/- 0.15 V bias over frequency sweep

www.manaraa.com

Figures 3.13 and 3.14 reveal the results of changing the applied bias from +/-0.05 mV to +/- 150 mV. With a zero and +/- 50 mV bias the peak frequency remains at 1275 MHz, however when the applied bias is changed to +/-150 mV a shift in the peak frequency to 1300 MHz is observed. It can be concluded from the behavior of the transponder that if a frequency discrimination scheme were to be implemented using this and other like devices, frequencies of operation may be desired (in this case, 1275 MHz) where both maximum and minimum output powers can be realized with a changing bias. The reason for this is that for modulation to occur for one particular transponder, essentially the signal needs to turn "off" and "on" as digital zeros and ones. It was observed that a zero bias and +/- 50 mV biases at 1275 MHz allowed signal transmission at a much higher output power and a +/- 150 mV bias at the same frequency caused the signal power to decrease by 15 dB.

A comparison of the performance characteristics of the 2nd generation transponder in a frequency sweep from 1265 MHz to 1315 MHz is shown in Figure 3.15 (output power) and Figure 3.16 (conversion efficiency); tabulated values are listed in Tables 3.2 and 3.3. The 0 V and +/- 50 mV bias settings exhibit relatively constant trends in conversion efficiency behavior, each providing maximum conversion efficiency at 1275 MHz. The +/- 150 mV bias settings, however, yield output powers from the transponder that are approximately 15 dB below that of the 0 V and +/- 50 mV bias settings. These combined results again verify feasibility of using the 2nd generation transponder for modulation purposes. A change in power output of 15 dB caused from only a 0.1 V difference in bias is sufficient to turn "on" and "off" the retransmitted signal.

62
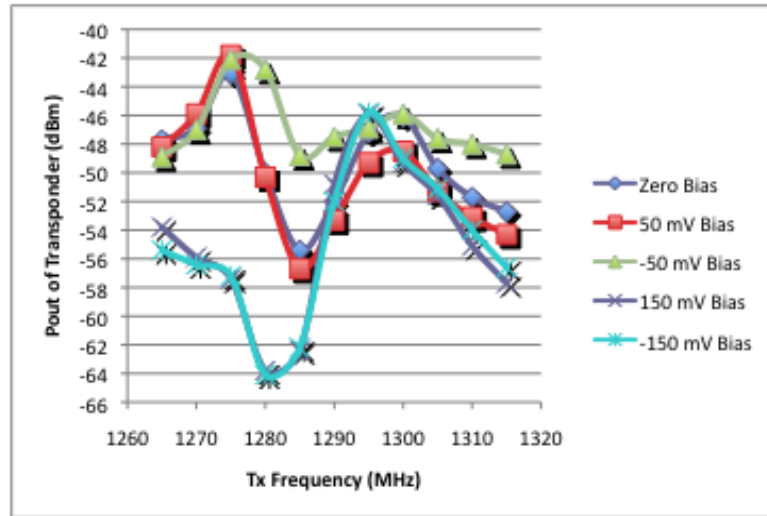
Figure 3.15: Comparison of P$_{out}$ of transponder at each tested bias over frequency sweep

Table 3.2: Comparison of P$_{out}$ of transponder at each tested bias over frequency sweep

Tx Frequency (MHz)	Pout of Transponder				
	0 V Bias	50 mV Bias	-50 mV Bias	150 mV Bias	-150 mV Bias
1265	-47.7	-48.2	-48.9	-53.8	-55.4
1270	-46.9	-45.9	-47	-55.9	-56.4
1275	-43.1	-41.8	-42.1	-57.4	-57.2
1280	-50	-50.3	-42.8	-63.8	-64.1
1285	-55.4	-56.7	-48.8	-62.4	-62.2
1290	-52	-53.3	-47.5	-50.8	-52
1295	-47.2	-49.3	-46.9	-45.9	-45.8
1300	-46.1	-48.5	-45.9	-49.3	-49
1305	-49.7	-51.3	-47.6	-51.6	-51.1
1310	-51.7	-53.1	-48	-55.1	-54
1315	-52.7	-54.3	-48.7	-57.7	-56.6

63
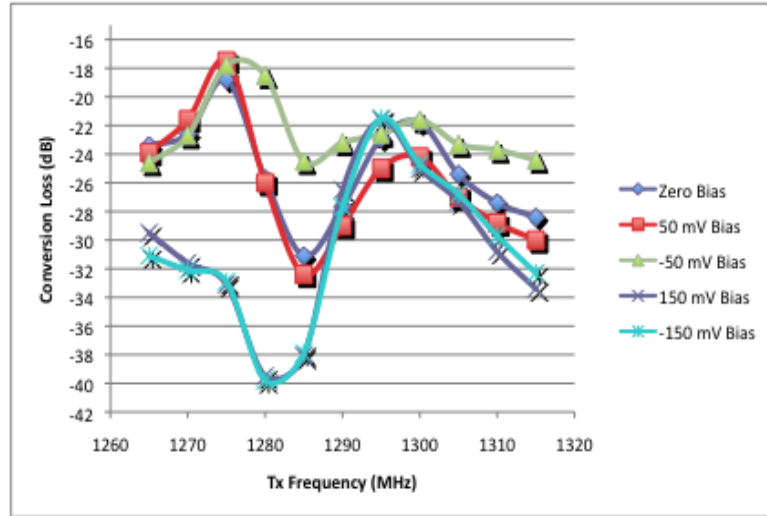
Figure 3.16: Comparison of conversion loss for each transponder at each tested bias over frequency sweep

Table 3.3: Comparison of conversion loss for each transponder at each tested bias over frequency sweep

Tx Frequency (MHz)	Conversion Loss of Transponder (dB)				
	0 V Bias	50 mV Bias	-50 mV Bias	150 mV Bias	-150 mV Bias
1265	-23.4	-23.9	-24.6	-29.5	-31.1
1270	-22.6	-21.6	-22.7	-31.6	-32.1
1275	-18.8	-17.5	-17.8	-33.1	-32.9
1280	-25.7	-26	-18.5	-39.5	-39.8
1285	-31.1	-32.4	-24.5	-38.1	-37.9
1290	-27.7	-29	-23.2	-26.5	-27.7
1295	-22.9	-25	-22.6	-21.6	-21.5
1300	-21.8	-24.2	-21.6	-25	-24.7
1305	-25.4	-27	-23.3	-27.3	-26.8
1310	-27.4	-28.8	-23.7	-30.8	-29.7
1315	-28.4	-30	-24.4	-33.4	-32.3

64

In the previous tests the transponder bias voltage was held constant while the transmitted frequency was swept. Measurements involving a sweep of the bias voltage needed to be made to determine the optimal biasing condition for operation of the transponder, as well as to verify with previous tests the conditions in bias voltage that would allow for modulation. Tests were performed at the previously determined optimal transmit frequencies of 1275 MHz and 1300 MHz with the same input power level to the transponder of -24.3 dBm. Bias voltage was swept from -0.3 V to 0.3 V and power output levels from the receiving antenna were recorded as shown in Figures 3.17 and 3.18.
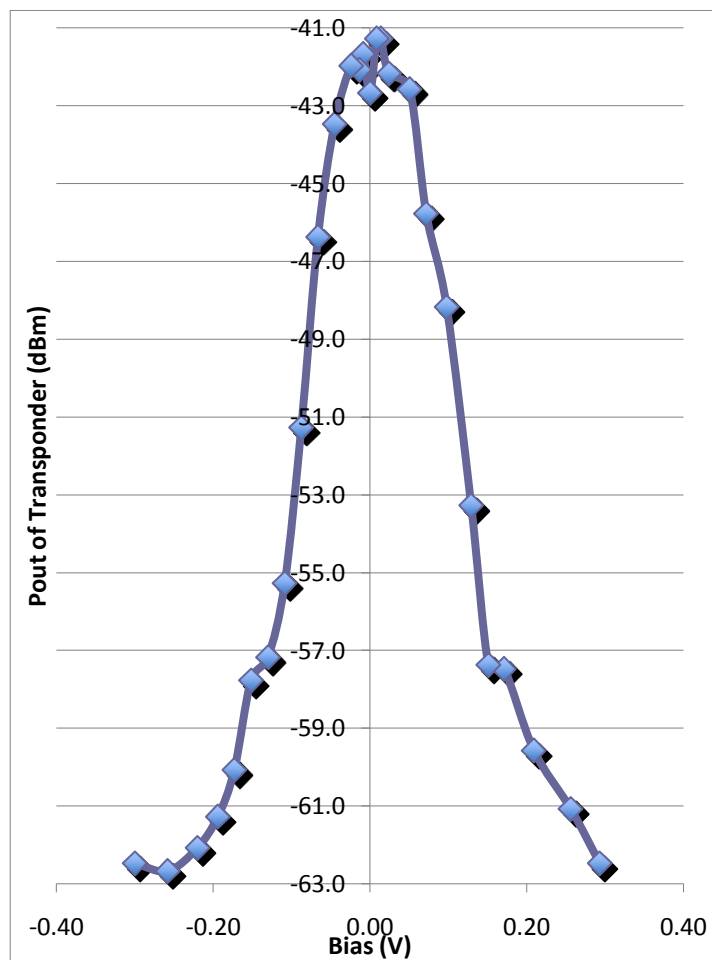
Figure 3.17: Bias vs. P_{out} of transponder at 1275 MHz T_x frequency

65

Analysis of the data in Figure 3.17 reveals the specific behavior of the biased diode transponder. The peak occurring at a bias voltage of approximately 0.01 V provides optimal performance of the transponder and the best conversion efficiency. Beginning with a bias of -0.3 V, output power from the transponder climbs steadily until it reaches -0.024 V, after which it fluctuates between -41 to -43 dBm, and then proceeds to sharply decline after 0.051 V. In a negative bias configuration, a change from -0.024 V to -0.13 V (Δ=0.106 V) produces a change in conversion loss of -20.7 dB (output power drops from 63.1 nW to 0.54 nW), which is sufficient to produce a digital logic zero in retransmission. Likewise, moving in the opposite direction, a change in bias from 0.009 V to 0.151 V (Δ=0.142 V) causes a change in conversion efficiency of -16.1 dB (output power drops from 74.1 nW to 1.82 nW), equally as sufficient to produce a digital logic zero.
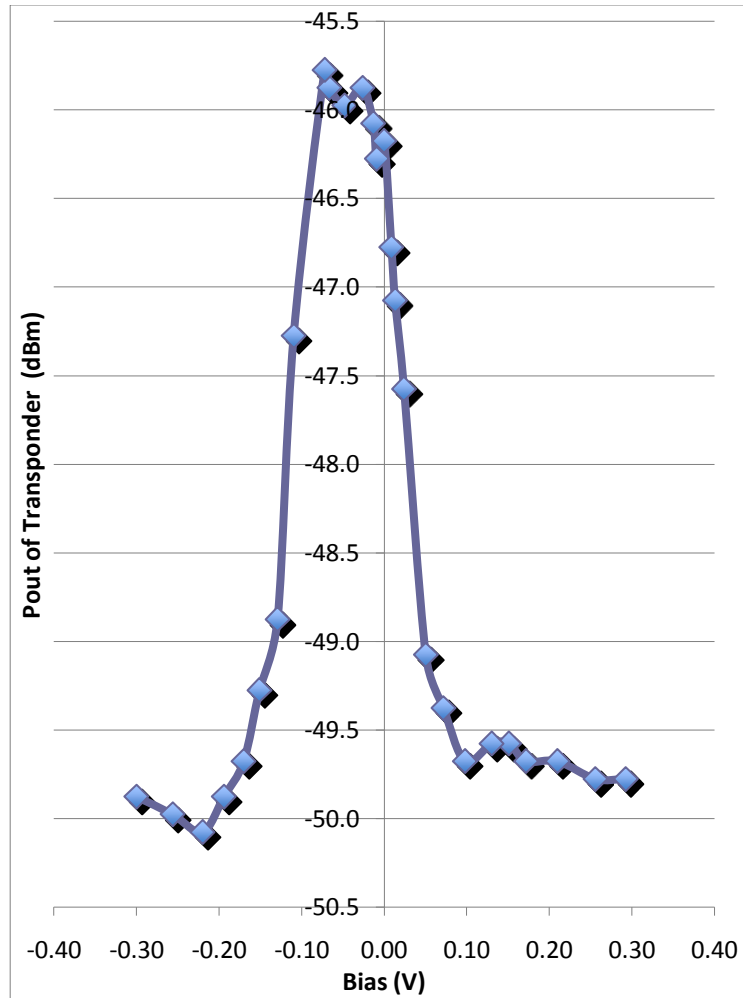
Figure 3.18: Bias vs. P_{out} of transponder at 1300 MHz T_x frequency

Analysis of the data in Figure 3.18 reveals the specific behavior of the biased diode transponder operating at 1300 MHz. As seen from the figure and correlating to Figure 3.15, the 2nd generation transponder operates less optimally at 1300 MHz. The peak output power occurring at 1300 MHz transmit frequency is -45.8 dBm, which is 4.5 dB less than the peak output power at a transmit frequency of 1275 MHz. Additionally, it is observed that a comparable change in bias that caused the results at 1275 MHz (Figure 3.17) has much less of an effect on output power of the transponder at 1300 MHz (Figure

67

3.18). In a negative bias configuration, a change from -0.072 V to -0.194 V (Δ=0.122 V) only produces a change in conversion loss of -4.1 dB (compared to -15.2 dB in Figure 3.17), which may not be sufficient to produce a clear digital logic zero in retransmission. Likewise, moving in the opposite direction, a change in bias from 0.0 V to 0.098 V causes a change in conversion efficiency of only -3.5 dB. This data verifies the results shown in Figure 3.15 where it can be seen that modulation is less likely possible at 1300 MHz due to much smaller fluctuations of amplitude from a change in bias. These characteristics are important when individual transponders are designed and fabricated for use in a sensing network employing frequency discrimination that is comprised of many devices. For the purposes of interrogation, each sensor would need to be identified by its frequency of operation.

3.7   Conclusions

The Remote Lock-In Amplifier concept was developed and tested. The capability to effectively communicate with the 1st generation low-power remote transponder within the RLIA system was demonstrated. A 2nd generation biased transponder was built to implement modulation of the retransmitted signal in an effort to employ frequency discrimination within a sensor network. Measurements of both transponders were compared and it was seen that application of the RLIA sensor system in a field environments is possible.

68

CHAPTER 4

APPLICATION OF RECTENNA TECHNOLOGY: DIODE-INTEGRATED RADAR DETECTOR

4.1   Introduction

The following chapter consists of the design, fabrication, and testing of a diode-integrated rectenna radar detector. The functionality of the radar detectors is to provide sensing capabilities for recognizing the presence of phenomena at a frequency of interest located at the remote sensor node, and correspondingly induce modulation to the signal being sent from the 2nd generation transponder to the interrogator node. Through this configuration, the complete RLIA system is realized for use in a frequency discrimination interrogation scheme.

Being essentially a rectenna, the radar detector senses microwaves occurring at a certain frequency within its local environment and transforms the microwave energy to a DC voltage proportional the strength of the signal impinging on the receiving antenna. The output of the radar detector can then be redirected to the bias input of the 2nd generation transponder, where this DC voltage input would cause a change in conversion loss, thus modulating the retransmitted interrogation signal to the base station. When the base station receives the modulated interrogation signal—using the lock-in amplifier—the information sensed by the radar detector will be extracted. However, when the radar detector is not sensing the presence of microwave energy at the frequency of interest it will simply have a zero DC voltage output, which will not affect the conversion

69

efficiency of the transponder. In a final realization of the RLIA system, the detector and transponder would both be incorporated as part of the remote sensor node.

4.2   Design of Radar Detector

As seen in Figure 1.4, the radar detector is designed by modifying the 1st generation transponder and replacing the transmitting 2.6 GHz patch antenna with a pad for a DC voltage connection. Also included in the design layout is a quarter-wavelength patch antenna operating at 1.3 GHz, a Schottky diode, and circuitry containing a 10 KΩ resistor for the purpose of maximizing voltage sensitivity and an 11pF RF blocking capacitor. The diode-integrated radar detector is fabricated on Taconic, 60 mil (Er=6.15) copper substrate incorporating surface mount components. A patch for soldering a DC wire connection is included after the DC blocking capacitor and shunt resistor.
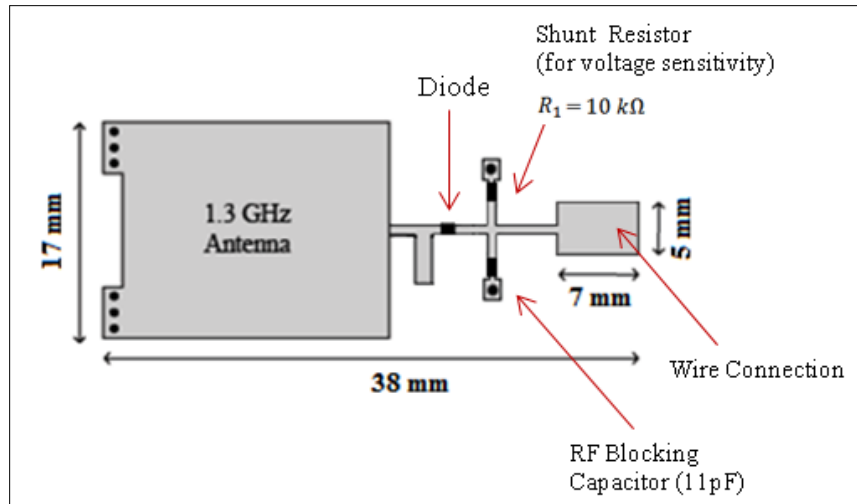
Figure 4.1: Layout of diode-integrated radar detector

Ideally, when the radar detector is employed in the RLIA system with the

transponder as part of an interrogation scheme using frequency discrimination, it will

sense phenomena occurring at a unique frequency from the interrogation signal being

sent to the transponder. However, for the purposes of this research, a frequency of

operation for the radar detector of 1300 MHz was chosen. This choice was made due to

ease of modifying the existing design of the transponder into the radar detector and taking

advantage of the previously existing narrow-band conjugate-matching technique used

with the 1st and 2nd generation transponders. By taking this approach, several advantages

were gained: the need for additional filtering for radar signal frequency-selection could

be minimized or eliminated as well as the need for discrete matching components, and

using 1300 MHz for the frequency of operation for the radar detector allowed verification

of the input power to the receive antenna of the transponder to be done. Additionally, due

to the compactness of the radar detector, it may be possible to integrate multiple devices

71

onto a single remote sensor node. This would provide the capacity to cover multiple frequencies at once or to harvest a higher amount of microwave energy at a single frequency. In the final realization of the RLIA system, where the remote sensor will be located in a field environment, the detector would be designed to operate at a different frequency, for example a frequency required for sensing the presence of two-way radio use. In Chapter Three it was observed that at the optimal operating frequency a change in bias of only 0.1 V could cause output power from the transponder to change by 15 dB, and it was concluded that this kind of change in conversion efficiency is sufficient to essentially turn "off" and "on" the retransmitted signal from the transponder.

4.3   Simulations of Radar Detector

Simulations of the diode-integrated radar detector were performed in Agilent ADS and the results of presented in this section. Figure 4.2 shows the schematic for the radar detector including the equivalent circuit models for the 1.3 GHz patch antenna (detector antenna), the Schottky diode based doubler (power detector), and the wire connection (output load). Referring to Figure 4.2, the detector antenna block is comprised of four impedance blocks (Z1P5, Z1P8, and Z1p9). Each impedance block provides the complex input impedance of the antenna at the fundamental frequency and 2nd through 4th harmonics. Immediately following each impedance blocks, in series, is an ideal band-pass filter that is open-circuited out-of-band. The band-pass filters guarantee that only one impedance block is active at a given harmonic. A full-wave analysis of the antenna was performed with conjugate-matching to the power detector at the radar signal frequency, which allowed values to be determined for simulation purposes. The detector

72

antenna is followed by a shunt stub for conjugate matching to the power detector, followed by the power detector. The power detector is comprised of a Schottky diode model, a shunt resister and shunt capacitor. The resistor is a 10 kΩ (Modelithics KOA 0402) model that provides maximum voltage sensitivity to the detector, and the capacitor is an 11pF (Modelithics Johanson 0402) model that behaves as an RF short. On the output side of the power detector is a high-value resistant load (1,000 Ω) for a DC voltage connection.
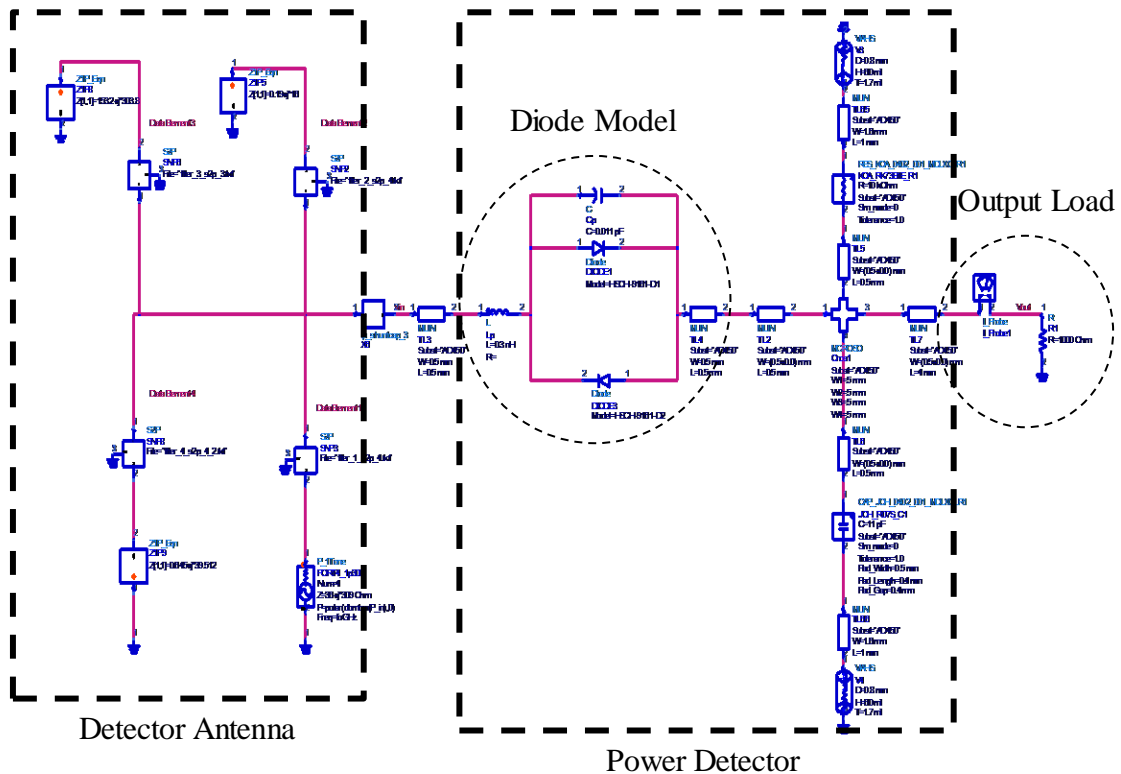
Figure 4.2: Schematic for the conjugate-matched radar signal detector

As seen in Figure 4.3, the simulated results of the radar detector design predicted an RF-to-DC conversion efficiency varying from ~0.02% to ~32% for an input power range of -55 dBm to -10 dBm. Additionally, simulation results verify that the radar detector design would be capable of inducing modulation onto the return signal sent from the 2nd generation transponder to the interrogating node.
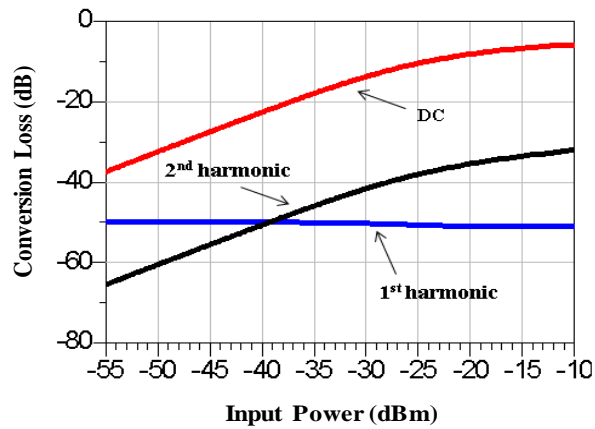
Figure 4.3: Simulated conversion efficiency of the radar signal detector
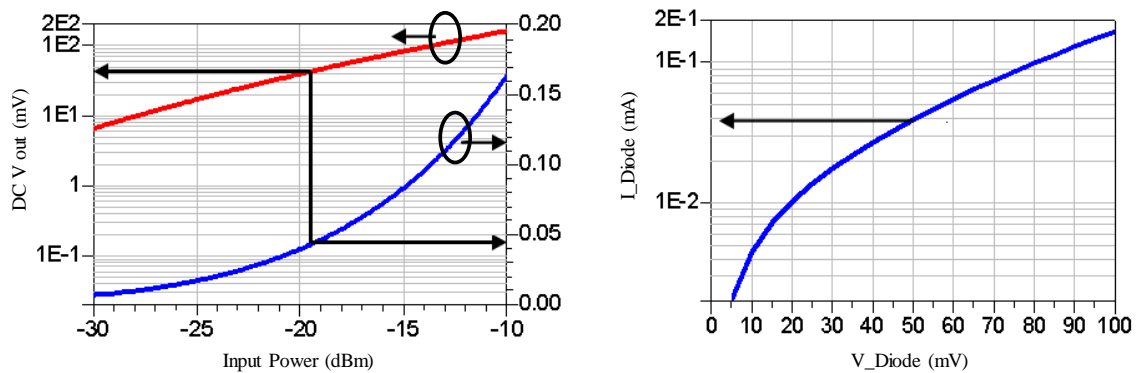
*Figure 4.4: Radar signal detector output voltage and current versus input power (left)
and I-V curve for the Schottky diode used in the multiplier
of the harmonic transceiver (right)*

74

Figure 4.4 (*left*) shows the V_{out} and I_{out} curves for the radar detector, and it is seen that with an input signal power of approximately -20 dBm an output of 50 mV at 50 μA is produced. The I-V curve in Figure 4.4 (*right*) indicates that these voltage and current conditions are sufficient to forward bias the diode doubler on the transponder. It can be concluded from the results of the simulations that if the presented radar detector was employed in a field environment for remote sensing, any signal greater than -20 dBm could be detected. The supplied bias from the detector due to this sensed signal would accordingly provide the required change in bias to the transponder that is needed to communicate back to the interrogating base station relevant information in the form of a modulated return signal.

4.4   Measurement Results of Radar Detector

To perform measurements of the radar detector the same standard testing equipment was used as was previously for testing the transponder (Table III, Appendix A). A distance of 4 feet was used to achieve an input power to the receiving antenna of the radar detector of -24.3 dBm. The input power to the receiving antenna is equal to the input power of the detector itself due to the fact that the receiving antenna gain is 0 dB. A block diagram of the testing configuration for the measurements of the radar detector can be seen in Figure 4.5. The transmitting antenna sends a 1.3 GHz signal modulated with a 1 kHz sine wave, which is again the chopping frequency that the lock-in amplifier will use for detection of the very small DC voltages at the output of the radar detector. A function generator is used to provide the reference frequency to the lock-in amplifier that matches the chopping frequency imparted onto the transmitted signal.

75
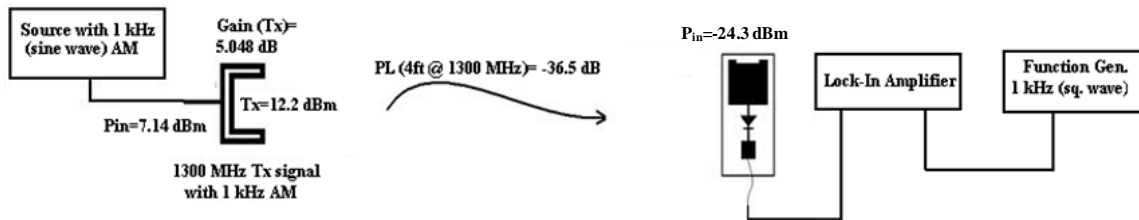
Figure 4.5: Block diagram of testing configuration of the radar detector

The first set of measurements of the radar detector involved a transmit power sweep beginning at the maximum calibrated source output of 12.2 dBm (input power of -23.4 dBm to the radar detector), and decreasing in 1 dB steps until the minimum detectable output from the radar detector is reached. The measured and simulated results are shown in Figure 4.6 (Table II, Appendix A), where it is seen that very good agreement was reached between these sets of data. Beginning with a -24.3 dBm power input to the detector, output voltage is approximately 20.5 mV (19.4 mV in simulation). As transmit power is decreased in 1 dB steps, output voltage is seen to decrease approximately according to $V_{out} \sim V_0{}^2 \sim P_{in}$, which is in accordance to the square-law region described in section 2.3 of Chapter Two. This square-law behavior exists until input power reaches approximately -45 dBm, after which point the voltage output from the radar detector is less stable. The reason for this instability is due to TSS of the detector, as discussed in section 3.3 of Chapter Three. However, in comparison to the DC voltage output of the Narda detector (Figure 3.3), the radar detector is seen to detect lower input powers within the square-law region. The Narda detector is seen to operate within the square-law region only until approximately -35 dBm, which is 10 dB above the edge of the square-law region for the radar detector.

76
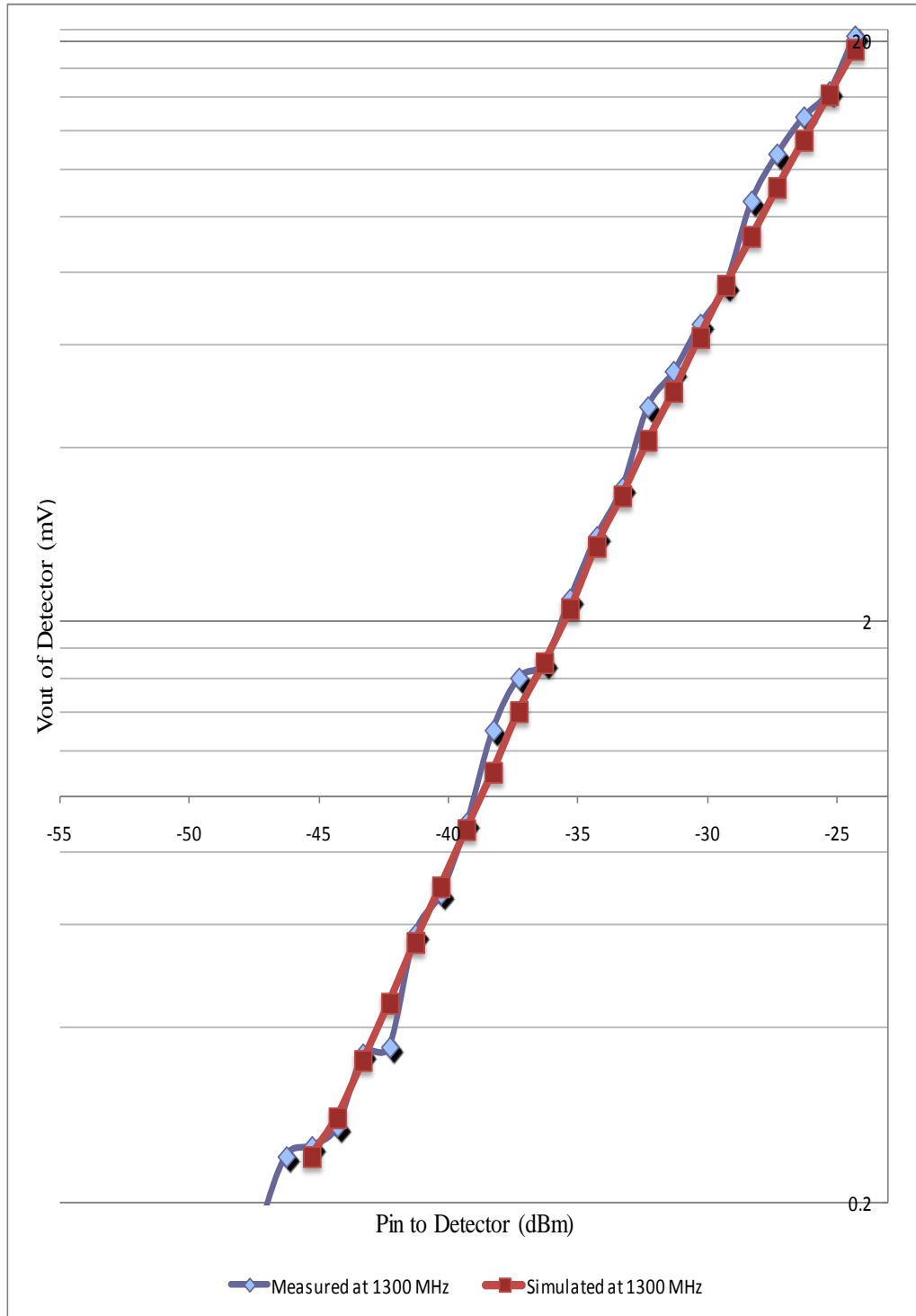
Figure 4.6: Measured vs. simulated results of the radar detector at P_{Tx} = 1300 MHz.

A comparison of the output voltage provided by the radar detector to the output voltage provided by the Narda detector (Figures 3.3, 4.6, and Appendix A) at an input power of approximately -45 dBm show that the radar detector has better performance characteristics, which are helpful within the proposed application. At an input power of -45.4 dBm, the Narda detector provides 0.069 mV of DC voltage at its output. The radar detector, however, provides 0.25 mV of DC voltage at its output with an input power of -45.3 dBm, which is approximately 360 percent of what the Narda detector can provide with this input power. This is a useful quality for the purposes of providing sufficient DC voltage biases to the transponder when smaller detected signals are present. To consider the feasibility of combining the radar detector and transponder together at the remote sensor node it is necessary to observe, as seen in Figure 3.17, that an approximate 40 mV change in bias was sufficient to provide a change in P_{out} of the retransmitted signal equal to -7.8 dB. To determine the required input power to the radar detector to produce an output DC voltage of 40 mV, it is possible to calculate the reponsivity of the radar detector, which is defined as $R = \frac{V_{out\,(mV)}}{P_{in}(mW)}$ and extrapolate from this value. The resistivity of the detector was found to be $5518.2 \frac{mV}{mW}$, therefore it was found that an input power to the radar detector of -20.4 dBm would be sufficient to produce an output DC voltage of 40 mV, which could ultimately be redirected to the bias of the transponder and induce amplitude modulation.

78

4.5   Conclusions

Design simulations in Agilent ADS and testing results of the radar detector were included to demonstrate minimum signal detection capabilities at 1300 MHz. It was seen that the fabricated radar detector was capable of sensing a signal of approximately -53 dBm, and accordingly producing a rectified DC voltage output of 0.05 mV. By calculating the responsivity of the radar detector, it was also discovered that an input power of -20.4 dBm to the device would be sufficient in creating enough DC voltage to modulate the transponder's return interrogation signal. Referring to the measurements presented in Chapter Three of the 2nd generation transponder in a bias sweep configuration (Figure 3.17), it is seen that an approximate 40 mV change in bias was sufficient to cause a 7.8 dB drop in conversion efficiency.

CHAPTER 5

SUMMARY AND RECOMMENDATIONS FOR FUTURE WORK

5.1 Summary

This thesis presented the research, design and fabrication associated with a unique application of rectenna technology combined with lock-in amplification. An extremely low-power harmonic transponder is conjoined with an interrogator base-station, and utilizing coherent demodulation the Remote Lock-In Amplifier (RLIA) concept is realized. The lock-in amplifier performs phase sensitive detection using a phase locked loop and reference frequency that is matched to the experimental signal's modulating frequency. The lock-in amplifier provides benefit to the interrogation system through its ability to detect signals below the noise floor by singling out signal components at specific reference frequencies. Without phase sensitive detection, extremely weak signals or signals arriving in the presence of an excessive amount of noise would otherwise be obscured.

Development of the RLIA began with a bench-top configuration including standard test equipment to perform characterization of a Narda 4503-01 coaxial Schottky barrier diode detector (Figure 3.2). The purpose of this testing was to verify both the functionality of the lock-in amplifier as well as sensitivity of the diode detector. Sensitivity was measured and results were found to correlate to the manufacturer's data sheet. Data related to detector sensitivity served as a reference for future measurements.

80

Using the sensitivity graph (Figure 3.3) and measured output voltage from the detector during experimentation with the full RLIA system, detector input power levels could be deduced, thus validating link budgets.

After characterizing the coaxial detector and verifying functionality of all testing equipment, a complete configuration of the RLIA system was constructed including the 1st generation remote transponder (Figure 3.7). Utilizing harmonic re-radiation with very low-power input, the 1st generation transponder (Figure 3.4) detects a transmitted interrogation signal and responds by retransmitting the second harmonic of the signal. The 1st generation transponder performs this task while using no additional power besides that which accompanies the wireless signal. Demonstration of the first complete configuration provided proof of concept for the RLIA and feasibility of processing relevant information under "zero" power operating conditions with a remote transponder. A spectrum analyzer and lock-in amplifier were used in the measurements and the data was compared (Figure 3.8). Results showed that the configuration including the lock-in amplifier provided detection of the return signal occurring below the noise floor (~5 dB below what was possible using a spectrum analyzer), thus verifying prior assertions of the RLIA.

Following the initial demonstration of the RLIA system, design and fabrication of a new version of the transponder was introduced. The existing zero-bias transponder was modified to include a modulating DC bias to the diode-based frequency doubler. Applied bias voltage directly changed the impedance match between the receiving 1.3 GHz antenna and the diode—by changing the diode impedance—causing a change in conversion loss. It was shown through testing that a change in conversion loss induces an

81

amplitude modulating effect on the retransmission of the signal from the transponder (Figure 3.15). A test of bias sweep at the optimal operating frequency was performed on the 2nd generation transponder and it was seen that a change of $\sim$ 0.1 V in either a positive or negative bias configuration induced an approximate 15 dB change in transponder output power (Figure 3.16). This performance characteristic can be advantageously used in implementing a frequency discrimination interrogation scheme for remote sensor networks.

Chapter Four of this thesis consisted of the research associated with and design of a radar detector. The radar detector was comprised of a quarter-wavelength patch antenna operating at 1.3 GHz, a Schottky diode, and circuitry containing a 10 KΩ resistor to maximize voltage sensitivity and an 11 pF RF blocking capacitor (Figure 4.1). The radar detector was designed to sense microwaves occurring at a certain frequency within its local environment and transform the microwave energy to a DC voltage proportional the strength of the signal impinging on its receiving antenna. The output of the radar detector could then be redirected to the bias input of the 2nd generation transponder, where this DC voltage input would cause a change in conversion loss and modulate the retransmitted interrogation signal from the transponder to the base station. When the base station receives the modulated interrogation signal the information sensed by the radar detector is extracted. When the radar detector is not sensing the presence of microwave energy at the frequency of interest, the conversion efficiency of the transponder will not be affected and the interrogating base station will not receive any information.

Design simulations in Agilent ADS and testing results of the radar detector were included to demonstrate minimum signal detection capabilities at 1300 MHz. It was seen

that the fabricated radar detector was capable of sensing a signal of approximately -53.3 dBm. Additionally, it was found that an input power of -20.4 dBm to the radar detector would accordingly produce a rectified DC voltage output of 40 mV. Referring to the measurements presented in Chapter Three of the 2nd generation transponder in a bias sweep configuration (Figure 3.17), it was seen that an approximate 40 mV change in bias was sufficient to cause a 7.8 dB drop in conversion efficiency. These two sets of data verified the feasibility of pairing the radar detector and the 2nd generation transponder together at the remote sensor node to perform modulation of interrogation signals.

5.2   Recommendations for Future Work

The future work of the Remote Lock-In Amplifier concept should involve advances in both the remote transponder (sensor node) and interrogating base station (interrogator node). Future research on the sensor node will be directed toward developing (1) "zero-power" sensors and (2) "low-power" sensors that will possess specific operational characteristics and optimized functionalities, demonstrating increased capability within a network. Efforts will be directed at increased power efficiency of the remote sensors to provide extremely long lifetimes with enhanced sensing and potential on/off functionality.

Continued development on the interrogator node will be aimed toward increasing compactness and evolving the bench-top interrogator/receiver that was demonstrated in this work to a compact hand held or portable device that communicates with sensor nodes. Some expected advantages of the next generation interrogation node over the bench-top version will be (1) the ability to simultaneously interrogate multiple sensor

83

nodes, and (2) the ability to communicate with other interrogator nodes to optimize

network quality of service. Overall future research will be focused on a primary goal of

optimally combining multiple interrogators with multiple low-power or zero-power

sensors.

REFERENCES

[1]   Brown, W.C.; , "The History of Power Transmission by Radio Waves," *Microwave Theory and Techniques, IEEE Transactions on* , vol.32, no.9, pp. 1230- 1242, Sep 1984

[2]   Presas, S.M.; Weller, T.M.; Silverman, S.; Rakijas, M.; , "High efficiency diode doubler with conjugate- matched antennas," *Microwave Conference, 2007. European*, vol., no., pp.250-253, 9-12 Oct. 2007

[3]   Bernhard, J.T.; Hietpas, K.; George, E.; Kuchima, D.; Reis, H.; , "An interdisciplinary effort to develop a wireless embedded sensor system to monitor and assess corrosion in the tendons of prestressed concrete girders," *Wireless Communication Technology, 2003. IEEE Topical Conference on* , vol., no., pp. 241- 243, 15-17 Oct. 2003

[4]   Hagerty, J.A.; Helmbrecht, F.B.; McCalpin, W.H.; Zane, R.; Popovic, Z.B.; , "Recycling ambient microwave energy with broad-band rectenna arrays," *Microwave Theory and Techniques, IEEE Transactions on* , vol.52, no.3, pp. 1014- 1024, March 2004

[5]   Le, T.; Mayaram, K.; Fiez, T.; , "Efficient Far-Field Radio Frequency Energy Harvesting for Passively Powered Sensor Networks," *Solid-State Circuits, IEEE Journal of* , vol.43, no.5, pp.1287-1302, May 2008

[6]   Jiawei Xu; Guy Meynants; Merken, P.; , "Low-power lock-in amplifier for complex impedance measurement," *Advances in sensors and Interfaces, 2009. IWASI 2009. 3rd International Workshop on* , vol., no., pp.110-114, 25-26 June 2009

[7]   Jung-Hwan Choi; Jung-Ick Moon; Seong-Ook Park; , "Measurement of the modulated scattering microwave fields using dual-phase lock-in amplifier," *Antennas and Wireless Propagation Letters, IEEE* , vol.3, no., pp. 340- 343, 2004 doi: 10.1109/LAWP.2004.839629

[8]   Davies, R.; Meuli, G.; , "Development of a digital lock-in amplifier for open-path light scattering measurement," *Industrial Electronics & Applications (ISIEA), 2010 IEEE Symposium on* , vol., no., pp.50-55, 3-5 Oct. 201045

[9]   Stanford Research Systems Application Note 3, "About Lock-In Amplifiers."

[10]   C. A. Balanis, Antenna Theory: Analysis and Design, 2nd edition, Wiley, N.Y., 1997

[11]   D. M. Pozar, Microwave Engineering, 3rd edition, Wiley, N.Y., 2005

[12]   Brown, W. C.; Kim, C. K.; , "Recent Progress in Power Reception Efficiency in a Free-Space Microwave Power Transmission System," *Microwave Symposium Digest, 1974 S-MTT International* , vol.74, no.1, pp. 332- 333, Jun 1974

[13]   Walsh, C.; Rondineau, S.; Jankovic, M.; Zhao, G.; Popovic, Z.; , "A conformal 10 GHz rectenna for wireless powering of piezoelectric sensor electronics," *Microwave Symposium Digest, 2005 IEEE MTT-S International* , vol., no., pp. 4 pp., 12-17 June 2005

[14]   Selvakumaran, R.; Liu, W.; Boon-Hee Soong; Luo Ming; Sum, Y.L.; , "Design of low power Rectenna for wireless power transfer," *TENCON 2009 - 2009 IEEE Region 10 Conference* , vol., no., pp.1-5, 23-26 Jan. 2009

[15]   Aguilar, S.M.; Weller, T.M.; , "Tunable harmonic re-radiator for sensing applications," *Microwave Symposium Digest, 2009. MTT '09. IEEE MTT-S International*, vol., no., pp.1565-1568, 7-12 June 2009

[16]   Tesla, N.; ""The Transmission of Electrical Energy without Wires," *Electrical World and Engineer,* March 5, 1904.

[17]   Matsumoto, H.; , "Research on solar power satellites and microwave power transmission in Japan," *Microwave Magazine, IEEE* , vol.3, no.4, pp. 36- 45, Dec 2002

[18]   Brown, W.C.; , "Experiments Involving a Microwave Beam to Power and Position a Helicopter," *Aerospace and Electronic Systems, IEEE Transactions on*, vol.AES-5, no.5, pp.692-702, Sept. 1969

[19]   Shinohara, N.; Matsumoto, H.; , "Experimental study of large rectenna array for microwave energy transmission," *Microwave Theory and Techniques, IEEE Transactions on* , vol.46, no.3, pp.261-268, Mar 1998

[20]   Shinohara, N.; Miyata, Y.; Mitani, T.; Niwa, N.; Takagi, K.; Hamamoto, K.; Ujigawa, S.; Jing-Ping Ao; Ohno, Y.; , "New application of microwave power transmission for wireless power distribution system in buildings," *Microwave Conference, 2008. APMC 2008. Asia-Pacific* , vol., no., pp.1-4, 16-20 Dec. 2008

[21]   R. H. George, "Solid state Power Rectifications," in E. C. Okress, Editor, *Microwave Power Engineering,* vol. 1, New York: Academic Press, 1968, pp. 275-294.

[22]   Brown, William C., George, Roscoe H. et al., U.S. Patent 3434678, March 25, 1969.

[23]   Brown, W.C., "The Combination Receiving Antenna and Rectifier," Microwave Power Engineering, vol. II, E. C. Okress, Ed. New York: Academic, 1968, pp. 273-275.

[24]   Brown, W.C.; , "An experimental low power density rectenna," *Microwave Symposium Digest, 1991., IEEE MTT-S International* , vol., no., pp.197-200 vol.1, 10-14 Jul 1991

[25]   Glaser, P.E.; , "The potential of satellite solar power," *Proceedings of the IEEE* , vol.65, no.8, pp. 1162- 1176, Aug. 1977

[26]   Glaser, P.E.; , "An overview of the solar power satellite option," *Microwave Theory and Techniques, IEEE Transactions on* , vol.40, no.6, pp.1230-1238, Jun 1992

[27]   Brown, W. C.; , "Electronic and Mechanical Improvement of the Receiving Terminal of a Free-Space Microwave Power Transmission System," Raytheon Contractor Rep. PT-4964, NASA CR-135194, Aug. 1977.

[28]   Brown, W.C.; Eves, E.E.; , "Beamed microwave power transmission and its application to space ," *Microwave Theory and Techniques, IEEE Transactions on*, vol.40, no.6, pp.1239-1250, Jun 1992

[29]   McSpadden, J.O.; Little, F.E.; Duke, M.B.; Ignatiev, A.; , "An in-space wireless energy transmission experiment," *Energy Conversion Engineering Conference, 1996. IECEC 96. Proceedings of the 31st Intersociety* , vol.1, no., pp.468-473 vol.1, 11-16 Aug 1996

[30]   STS-80 Columbia ORFEUS-SPAS-2/Wake Shield Facility-3, KSC Release No. 124-96, October 1996, NASA; http://wwwpao.ksc.nasa.gov/kscpao/release/1996/124-96.htm

[31]   Matsumoto, H.; "Microwave power transmission from space and related nonlinear plasma effects," *Radio Sci. Bull.*, vol. 273, pp. 11-35, June 1995.

[32]   Shinohara, N.; , "Development of high efficient phased array for microwave power transmission of Space Solar Power Satellite/Station," *Antennas and Propagation Society International Symposium (APSURSI), 2010 IEEE* , vol., no., pp.1-4, 11-17 July 2010

[33]   Powercast Corporation; web address: http://www.powercastco.com/; Feb 17, 2011.

[34]   WiTricity; web address: http://www.witricity.com/index.html; Feb 17, 2001.

[35] Wireless Power Consortium; web address: http://www.wirelesspowerconsortium.com/; Feb 17, 2001.

[36] Strassner, B.; Kai Chang; , "A circularly polarized rectifying antenna array for wireless microwave power transmission with over 78% efficiency," *Microwave Symposium Digest, 2002 IEEE MTT-S International* , vol.3, no., pp.1535-1538, 2002

[37] Ali, M.; Yang, G.; Dougal, R.; , "A new circularly polarized rectenna for wireless power transmission and data communication," *Antennas and Wireless Propagation Letters, IEEE* , vol.4, no., pp. 205- 208, 2005

[38] Lim, S.; Leong, K.M.K.H.; Itoh, T.; , "Adaptive power controllable retrodirective array system for wireless sensor server applications," *Microwave Theory and Techniques, IEEE Transactions on* , vol.53, no.12, pp. 3735- 3743, Dec. 2005

[39] Lim, S.; Itoh, T.; , "A 60 GHz retrodirective array system with efficient power management for wireless multimedia sensor server applications," *Microwaves, Antennas & Propagation, IET* , vol.2, no.6, pp.615-625, Sept. 2008

[40] Olgun, U.; Chi-Chih Chen; Volakis, J.L.; , "Low-profile planar rectenna for batteryless RFID sensors," *Antennas and Propagation Society International Symposium (APSURSI), 2010 IEEE* , vol., no., pp.1-4, 11-17 July 2010

[41] Benes, E.; Groschl, M.; Seifert, F.; Pohl, A.; , "Comparison between BAW and SAW sensor principles," *Ultrasonics, Ferroelectrics and Frequency Control, IEEE Transactions on* , vol.45, no.5, pp.1314-1330, Sep 1998

[42] Wilson, W.C.; Malocha, D.C.; Kozlovski, N.; Gallagher, D.R.; Fisher, B.; Pavlina, J.; Saldanha, N.; Puccio, D.; Atkinson, G.M.; , "Orthogonal Frequency Coded SAW Sensors for Aerospace SHM Applications," *Sensors Journal, IEEE* , vol.9, no.11, pp.1546-1556, Nov. 2009

[43] Pohl, A.; Seifert, F.; , "Wirelessly interrogable SAW-sensors for vehicular applications," *Instrumentation and Measurement Technology Conference, 1996. IMTC-96. Conference Proceedings. 'Quality Measurements: The Indispensable Bridge between Theory and Reality'., IEEE* , vol.2, no., pp.1465-1468 vol.2, 1996

[44] Kozlovski, N.Y.; Malocha, D.C.; , "SAW passive wireless multi sensor system," *Ultrasonics Symposium (IUS), 2009 IEEE International* , vol., no., pp.1541-1544, 20-23 Sept. 2009

[45] Aguilar, S.M.; Weller, T.M.; , "Tunable harmonic re-radiator for sensing applications," *Microwave Symposium Digest, 2009. MTT '09. IEEE MTT-S International* , vol., no., pp.1565-1568, 7-12 June 2009

88

[46]   A. D. Poularikas; S. Seely;, Signals and Systems, PWS Publishers, Boston, MA, 1985

[47]   Hewlett-Packard Application Note 923, "Schottky Barrier Diode Video Detectors."

[48]   Linli Xie; Yonghong Zhang; Yong Fan; Conghai Xu; Yuanbo Jiao; , "A W-band detector with high tangential signal sensitivity and voltage sensitivity," *Microwave and Millimeter Wave Technology (ICMMT), 2010 International Conference on* , vol., no., pp.582-531, 8-11 May 2010

89

APPENDICES

90

Appendix A   Additional Tables of Measurements, Lists and Specifications of Equipment

Table I: Sensitivity measurements of Narda detector (Model 4503-01)

Calibrated Power (dBm)	Vdc (mV)
11.58	586.7
10.58	521.5
9.58	460.5
8.58	406.7
7.58	356.4
6.58	314.3
5.58	274.3
4.58	239.3
3.58	207.3
2.58	180.5
1.58	154.7
0.58	133.3
-0.42	113.6
-1.42	96.0
-2.42	81.5
-3.42	68.9
-4.42	57.8
-5.42	48.0
-6.42	39.7
-7.42	33.1
-8.42	27.3
-9.42	23.2
-10.42	18.8
-11.42	15.3
-12.42	12.4
-13.42	10.06
-14.42	8.07
-15.42	6.49
-16.42	5.17
-17.42	4.16
-18.42	3.32
-19.42	2.73
-20.42	2.16
-21.42	1.74
-22.42	1.39
-23.42	1.12
-24.42	0.90
-25.42	0.73
-26.42	0.58
-27.42	0.48
-28.42	0.39

Table I: (Continued)

Calibrated Power (dBm)	Vdc (mV)
-29.42	0.33
-30.42	0.27
-31.42	0.23
-32.42	0.20
-33.42	0.17
-34.42	0.15
-35.42	0.13
-36.42	0.12
-37.42	0.11
-38.42	0.097
-39.42	0.092
-40.42	0.087
-41.42	0.082
-42.42	0.079
-43.42	0.080
-44.42	0.070
-45.42	0.069
-46.42	0.068
-47.42	0.069
-48.42	0.070
-49.42	0.069
-50.42	0.061
-51.42	0.061
-52.42	0.059
-53.42	0.061
-54.42	0.060
-55.42	0.059
-56.42	0.058
-57.42	0.059
-58.42	0.059
-59.42	0.062
-60.42	0.061
-61.42	0.060
-62.42	0.059
-63.42	0.059

Appendix A   (Continued)

Table II: Measured and simulated sensitivity values of radar detector

T_x Power (dBm)	P_{in} Radar Detector (dBm)	V_{DC} meas. (mV)	V_{DC} simul. (mV)
12.2	-24.3	20.5	19.4
11.2	-25.3	16.4	16.2
10.2	-26.3	14.8	13.5
9.2	-27.3	12.8	11.2
8.2	-28.3	10.6	9.2
7.2	-29.3	7.6	7.6
6.2	-30.3	6.5	6.2
5.2	-31.3	5.4	5
4.2	-32.3	4.7	4.1
3.2	-33.3	3.4	3.3
2.2	-34.3	2.8	2.7
1.2	-35.3	2.2	2.1
0.2	-36.3	1.7	1.7
-0.8	-37.3	1.6	1.4
-1.8	-38.3	1.3	1.1
-2.8	-39.3	0.9	0.88
-3.8	-40.3	0.68	0.7
-4.8	-41.3	0.58	0.56
-5.8	-42.3	0.37	0.44
-6.8	-43.3	0.36	0.35
-7.8	-44.3	0.27	0.28
-8.8	-45.3	0.25	0.24
-9.8	-46.3	0.24	0.18
-10.8	-47.3	0.18	0.14
-11.8	-48.3	0.12	0.11
-12.8	-49.3	0.08	0.09
-13.8	-50.3	0.05	0.07
-14.8	-51.3	0.04	0.06
-15.8	-52.3	0.06	0.05
-16.8	-53.3	0.05	0.04

Table III: List of parts used in testing configuration

| Manufacturer:	Model and Specs:	Equipment Type:
Hewlett Packard	8594E (9k – 2.9 GHz)	Spectrum Analyzer
Stanford Research Systems	SR530	Lock-In Amplifier
Agilent	33120A (15 MHz)	Function Generator
Agilent	ESG-D4000A (250 kHz – 4 GHz)	Signal Generator
Narda	4503-01	Schottky Barrier Detector
Narda	614A (2.6 – 3.95 GHz, Gain=5.048 dBi)	Waveguide
Sciperio	(custom made = 1.3 GHz, Gain=7.075 dBi)	Waveguide
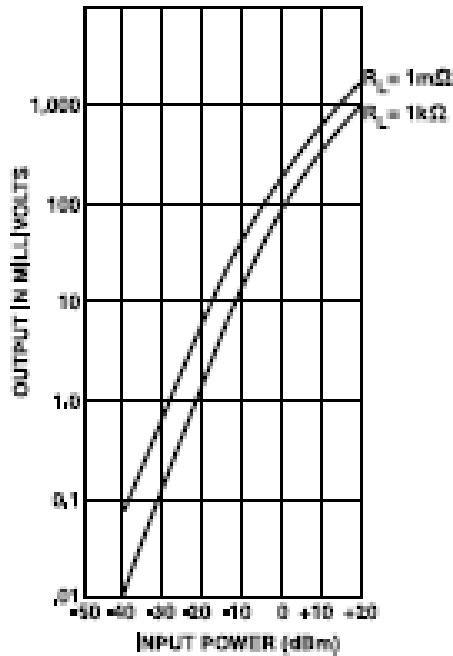
Figure I: Sensitivity curve of Narda Schottky-barrier detector (4503-01)

Appendix B   1st Generation Transponder Measurement Notes

The following summarizes the challenges confronted during testing of the 1st generation transponder within the RLIA set-up and techniques of overcoming them.

B.1 Transmitter Block

It was known that a properly functioning 1st generation transponder had a peak conversion efficiency of around -20 dB, occurring at input power levels within the range of approximately -30 dBm to -20 dBm. Also known, was that as the input power to the transponder falls below -30 dBm the conversion efficiency also starts to decrease. The same effect occurs when the input power to the transponder reaches above -20 dBm. Simply sending more transmit power from the interrogator was not the solution to maximizing the retransmitted 2.6 GHz signal power from the transponder. Testing had to be done to insure that the transmitted 1.3 GHz signal was between -20 dBm and -30 dBm and that it was also a clean transmit signal, free of harmonics.

The first part of testing included the front-end receiver block as seen in Figure 3.7 (not include the down-conversion stage). To accomplish a clean transmit signal, first a low-pass filter (VLF-1800+) was added between the signal source and the transmitting antenna. However signal harmonics were still seen on the spectrum analyzer at the receiving end of the system. Investigation needed to be done to see if the signal harmonics were originating from the signal source. It was estimated that the total path loss from transmitting antenna to receive antenna including the conversion loss of the transponder was close to 100 dB. Therefore, any signal harmonics originating from the signal source needed to be suppressed by at least this value. It was found that as 3-5

95

Appendix B   (Continued)

successive filters were added in series, the transmitted signal was not sufficiently clean.

However introducing 7 VLF-1800+ filters in series provided a transmit signal that was

sufficiently free of source generated harmonics to achieve a clean received signal at 2.6

GHz. This however, was not in itself sufficient for a clean receive signal from the

transponder. In addition work had to be done to the receiver side of the interrogator.

B.2 Receiver Block

In addition to introducing filters at the transmit end of the RLIA system,

additional filtering became required to eliminate interference signals from entering the

system. Not only were 2.6 GHz coaxial band-pass filters (VBFZ-2527+) required for

filtering interference signals, as seen in Figure 3.7, they were also required for

eliminating harmonics caused by the amplifiers within the receiver block, as well as

harmonics created from non-linear behavior of the spectrum analyzer. In addition to the

coaxial band-pass filters, a coupled-line band-pass filter (percent bandwidth = 1%) was

designed to narrow the noise bandwidth of the system. The coupled-line band-pass filter

was not by itself successful at narrowing the noise bandwidth. During testing, it was seen

that the filter was behaving as antenna and was itself introducing interference signals into

the system. To overcome this, a metal enclosure was utilized to house the filter and block

additional interference from being injected into the system at the receiver block end.

After this measure was taken, the receive signal seen on the spectrum analyzer was

greatly improved.

96

A down-conversion stage with an IF of 61 MHz was implemented to eliminate unwanted signals that were appearing around 2.6 Ghz. Eliminating these interference signals was not crucial in terms of viewing the signal on the spectrum analyzer, because the desired received signal can be visually identified from the interference signals. However, proper filtering of interference is necessary for the purposes of reading voltage levels on the lock-in amplifier. The total power being input to the detector will provide a voltage reading to the lock-in amplifier, and if this total power input is not solely comprised of the desired signal, the lock-in amplifier will give an inaccurate reading. It was found that the combination of the transmit signal filtering, added receiver block filtering and additional down-conversion was sufficient to eliminate unwanted signals at the desired frequencies.